FOREST FIRE HAZARD MAPPING IN THE LA PEYNE AREA, FRANCE

MSC THESIS

Kevin Gortmaker
0428779

April 12th, 2010
revision: January 12th, 2011

Utrecht University
Faculty of Geosciences
Department of Physical Geography

PREFACE

This thesis, on forest fire hazard mapping, is written as the final part of a larger research project, which forms the closure of the Master-program "Physical Geography – Natural Hazards & Earth Observation" at the faculty of Geosciences, Utrecht University, the Netherlands.

The combination of literature review and research proposal served as the preparation and starting point for a field campaign of two months, in the La Peyne catchment - Southern France, during which the required field-data was collected. Finally, all data (both field observations and remotely sensed images) was analyzed at Utrecht University and resulted in this final thesis.

~~~~~~

Through many ups and downs, (the revision) of this thesis has been completed. Fire hazard has been a fun, but first and foremost challenging topic, in which many questions needed to be answered and in which, most likely, many questions are still left unanswered. Fire is as intriguing as it is fearsome: while many lives can be at stake when a wildfire shoots out of control, many ecosystems rely on the fires to return nutrients to their soils.

Creating maps of fire hazard is by no means limited to the ones created in this research, further studies and model developments will undoubtedly spawn a myriad of new ideas and applications.

All said and done; it has been a long, but interesting trip.

Kevin Gortmaker

January 12th, 2011
~~~~~~

ABSTRACT

Due to their potentially severe social and ecological effects, wildfires are an important topic for research, both in terms of their spreading behavior, and their chance of ignition. This research will emphasize the latter; the primary research objective is to create a fire hazard map for the chosen study area. To achieve this, the research focuses on creating four main components of such a map, using a combination of both in-field measurements and remotely sensed data:

1. Risk caused by vegetation
2. Risk caused by human activity
3. Risk caused by terrain
4. Risk caused by weather

Risk caused by vegetation was computed for each of the occurring fuel types encountered in the study area. The highest vegetation risk was shown to be in the pine forest and areas with large amounts of shrubs and ground fuels. The lowest risk values were associated with vegetation mainly consisting of mature trees which, due to their thicker trunks, would be less prone to wildfire ignition and/or spread.

Risk caused by human activity was concentrated along the (main) roads, dirt roads and hiking trails. The edges of villages, agricultural lands and parking lots (barbecue areas), indicate locations where sparks or still smoldering material may end up igniting the vegetation. Risk caused by terrain was determined by extracting slope and aspect from an existing digital elevation model. Risk caused by weather was omitted from the combined hazard map, due to poor data applicability on the valleys present in the study area.

The final, overall hazard map was created by combining the vegetation, human, and topographical risk maps into one, each with its own weight factor. The most severe hazards are found in the pine forest in the southeastern part of the study area, and to the west and south of the lake, where the vegetation mainly consists of high amounts of shrubs and woody fuel / litter. The immediate surroundings of buildings, parking lots and agricultural areas pose a strong increase in fire hazard due to increased risk of ignition from glowing embers or coals (barbecue, campfires).

The combination of several individual influences on fire hazard, into a single map, can provide insights into relationships between the factors themselves, and how they reinforce or perhaps weaken each other. Since overall fire hazard is ultimately determined by multiple factors, changing one of them could very well lead to the desired reduction of wildfires.

Object-orientated classification methods may help in classifying man-made structure from either satellite imagery or (existing) topographic maps. More insight is needed on the actual influence of aspect on overall fire risk. Maybe in future, a direct feed from meteorological systems can be used as an overlay on top of the combined hazard map, allowing areas that reach a certain hazard-threshold to be identified quicker and more accurately.

CONTENTS

All maps designed for A3 printing (1:25000)

Scale on A4 paper approx. 1:37000

1 INTRODUCTION

Forest fires (or more general: wildfires) are a critical factor of disturbance in worldwide ecosystems. Their potential social and ecological effects make them an important topic for research.

Depending on fire frequency, intensity and residence time, as well as on plant resilience, resistance and rejuvenation, forest fires will have different effects on soils and vegetation. Besides the physical and biological consequences, more and more interest is being shown for the economic and social impacts (loss of homes, lives) of wildfires.

Table 1.1 shows the total amount of burnt area, for five European Mediterranean countries, during the period 1980-2007. While economic damage is much more difficult to judge then physical and/or environmental damage, an estimate is given in table 1.2 for a single wildfire event, spanning only 417 hectares, in 2000 (Kumluca, Turkey). Dividing total costs by area affected would yield a roughly estimated cost of nearly $ 1000 per hectare burned.

Burnt area (ha)	**Portugal**	**Spain**	**France**	**Italy**	**Greece**	**Total**
2007	*31,450*	*82,048*	*8,570*	*227,729*	*225,734*	***575,531***
Yearly average (1980-1989)	73,484	244,788	39,157	147,150	52,417	**556,995**
Yearly average (1990-1999)	102,203	161,319	22,735	118,573	44,108	**448,938**
Yearly average (2000-2007)	174,544	136,411	25,052	87,387	53,485	**476,879**
Total (1980-2007)	**3,153,226**	**5,152,353**	**819,331**	**3,356,321**	**1,393,130**	**13,874,361**

TABLE 1.1 – BURNT AREA IN FIVE EUROPEAN MEDITERRANEAN COUNTRIES OVER BETWEEN 1980-2007. THE TOTAL OF 13,874,361 HA (138,743 KM^2) IS ROUGHLY EQUAL TO THE TOTAL SURFACE AREA OF GREECE (132,000 KM^2), OR HALF THE TOTAL SURFACE AREA OF ITALY (301,000 KM^2) . [*SOURCE: CARNIA ET AL., 2008]*

Damage type	**Value (USD)**
Timber damage	$ 129,991
Reforestation cost	$ 192,405
Extinguishing cost (machines etc.)	$ 45,268
Loss of land income (revenues)	$ 15,490
Alternative employment cost	$ 21,568
General administration cost	$ 5,922
Total damage value	**$ 410,644**

TABLE 1.2 – ESTIMATE OF ECONOMIC DAMAGE AS A RESULT OF A WILDFIRE EVENT IN 2000 (KUMLUCA, TURKEY), WHICH BURNED 417 HECTARES. *[TÜRKER, 2005]*

An important part in determining wildfire hazard for a certain area is the creation of so called fuel maps; maps that show the occurrence of different (combinations of) land coverage. In general, the classification of different fuel types focuses on rating the potential rate of spread, or rate of perimeter increase from an initiating fire, so that initial response time can be designed to contain the fire at a reasonable size (Sandberg *et al.*, 2007b). Each land cover type has specific properties, mostly concerning the present vegetation, that determine both the potential for a fire to start and how an existing fire will migrate through the area.

While the main application of such fuel maps is therefore found in simulating active wildfires, coupled with current meteorological data they are also a major contributor in predicting if, when and where a fire may start in the first place. Fuel maps can provide insights into where the likely major paths of fire spread will be, allowing urban communities close to wildland to take measures to reduce their fire hazard (Krasnow *et al.*, 2009). These measures can, among others, entail the removal of fuel by deliberately burning it in a controlled manner. The fuel maps can also be used in the prediction of smoke and CO_2 production of a wildfire (Keane *et al.*, 2000).

Besides ground and surface fuels, canopy fuels are a subject of increasing interest. A crown fire is a fire that burns in the (elevated) canopy fuels, and can cause wildfires to rapidly spread out over large areas. Van Wagner (1977 & 1993, in: Scott & Reinhardt, 2001) describes three types of crown fire that are generally recognized:

- *passive* crown fire (no spread, only isolated trees);
- *active* crown fire (spread, but still dependant on underlying surface fire);
- fully *independent* crown fire (self-supported spread).

From first to last, the three types of crown fire increase in hazard. Mostly in terms of risk for the surrounding vegetation to burn, but also in terms for people (living) in the affected area. If the moisture content is low enough, fire spread rates can substantially increase due to active (or even independent) crown fires, limiting the time window in which evacuation and/or fire fighting scenarios can be initiated.

1.1 FACTORS DETERMINING WILDFIRE HAZARD & BEHAVIOR

A wildfire can both ignite in, and spread through, the available ground, surface and/or crown fuels. While separate modeling of these two processes is possible, they are closely related: usually the prediction of fire behavior is based on rating the local (grid cell's) fire hazard. This means that, in essence, fire spread is based on the possibility that a neighboring location will catch on fire in the next time step. As a result, both fire hazard (risk of ignition) and fire spread models share most of their determining – and interacting – factors (Darmawan *et al.*, 2001; Grishin & Shipulina, 2002; Riaño *et al.*, 2002; Isabella Bovolo *et al.*, 2009):

1) availability of certain fuel types;
2) human activity;
3) terrain (slope and aspect);
4) weather.

These factors are discussed in more detail in the following sections.

1.1.1 FUEL TYPES

Fuel types are determined by vegetation properties such as size, density, age, litter production (e.g. leaves, needles) and species (Barrett *et al.*, 2007). The vertical arrangement of biomass, both on- and above-ground, dictates the intensity and severity of a fire, especially a crown fire (Keane *et al.*, 2000). Anderson (1982) defined four groups of vegetation in this respect. Grasses and shrubs are vertically orientated, and thus rapidly increase in layer-depth with increasing load. Timber litter and slash are horizontally orientated and increase in layer-depth slowly as the load increases.

A combination of different fuel types is known as a fuel model (Anderson, 1982). Merrill & Alexander (1987, in: Lanorte & Lasaponara, 2007) define a fuel model as *"an identifiable association of fuel elements of distinctive species, form, size, arrangement, and continuity that will exhibit characteristic fire behavior under defined burning conditions."* Darmawan *et al.* (2001) found that depending on local conditions, very different hazard levels can occur within one vegetation type and that, therefore, the state (health) and structure (layering) of the vegetation is more important than the specific vegetation species. Chuvieco & Congalton (1988, in: Darmawan *et al.*, 2001) reached a similar conclusion for Mediterranean regions.

1.1.2 HUMAN ACTIVITY

An increasingly important factor in wildfire hazard is human activity. More than 90% of wildfires (ignitions) in Spain and other European Mediterranean countries are caused by people (FAO, 2007 in: Martinez *et al.*, 2009). Most often, forest fires occur along man-made openings in forests, used for motorways, railroads and power lines (Grishin & Shipulina, 2002). Ignition sources could also be linked to the spatial arrangement of human dwellings and continuous vegetation (Syphard *et al.*, 2007, in: Lampin-Maillet *et al.*, 2009). Lampin-Maillet *et al.* go on to conclude that these differences in dwelling types should be combined with the fuel and terrain data to assess the overall fire hazard. They also state that the risk assessments could be improved by including other socio-economic factors such as distance to the nearest road and population density.

A more indirect human influence is logging (timber harvesting). Logging produces large amounts of easily combustible residues in many forested areas, possibly increasing fire hazard to unacceptable levels (Radloff *et al.,* 1982). Besides this immediate effect, Radloff *et al.* (1982) provide a timeline of increased fire hazard following the moment of logging. Slash (the logging residue which poses a high risk) will dominate a forest stand for 5 years after the harvest. During the next 35 years, brush (shrubs, characterizing the early development stage of a new forest stand) will determine the fire

behavior. After these first 40 years, the new mature trees will dominate the stand. Fire hazard is considerably lower, but still greater than that of the original, usually much older forest.

Human activities are very dynamic in time and space, making the recognition of specific spatial patterns difficult, for instance in the case of pyromania or other intentional motivations (Martinez *et al.*, 2009). Some factors however, such as the man made openings and villages mentioned above, campsites and picknick-areas, are indeed static features; they can be mapped as zones with a constant high risk of (unintentional) fire ignitions.

1.1.3 TERRAIN

While (mapping of) fuel type is by far the most documented factor in determining forest fire hazard, there are other static factors influencing fire behavior, such as slope and aspect of the terrain (Riaño *et al.*, 2002; Isabella Bovolo *et al.*, 2009). Because of rising hot air, a fire will expand quicker upslope than across a plain or down slope. Moisture content of the fuel determines the time it takes before it will ignite. Aspect is related to this in the sense that a southern facing slope will receive more solar heat than a north facing slope, causing the southern slope to dry quicker and thus having a lower fuel moisture content.

Because of the additional complexity caused by terrain conditions, assessing wildfire hazard by means of field observations alone is very tedious. Remotely sensed data is used more and more as a time (cost) effective method of data collection, especially where topographical properties are concerned.

1.1.4 WEATHER

Weather data are also an influencing factor in determining fire hazard and behavior. Meteorological factors that influence fire spread are wind speed, wind direction, temperature and relative humidity (Riaño *et al.*, 2002). The first two directly influence fire *spread*, on a (very) small timescale, as they physically interact with the flames themselves. Temperature and humidity influence fire *hazard*, and do so on a much larger timescale; only after a prolonged period of drought and heat will the risk increase significantly. A single, isolated hot or dry day will be of little consequence for the overall fire hazard. De Albuquerque *et al.* (2007) conclude that the medium value of dryness in the air determines the possibility of fire. They also verified that a high air-temperature was the main factor in a material burning in one area, while not burning in another.

1.2 RESEARCH OBJECTIVES

Due to their potentially severe social and ecological effects, wildfires are an important topic for research, both in terms of their spreading behavior, and their chance of ignition. This research will emphasize the latter; in this research, unless stated otherwise, risk is defined as the *risk of ignition*.

The primary research objective is to create a fire hazard map for a Mediterranean site prone to forest fires. Combining literature, fieldwork, remotely sensed imagery and GIS software, this research aims to answer the following questions:

1. *Can the wildfire risk, caused by vegetation (fuel type), be mapped by means of remote sensing?*

2. Roads, villages, power lines, agricultural plots and other locations associated with human activity are considered to influence fire hazard. *Can the risk posed by these human activities be mapped by means of remotely sensed and/or (thematic) topographical data?*

3. *Can the risk caused by the (static) terrain properties of slope and aspect, be adequately mapped by deriving them from existing elevation maps?*

4. Fuel types, terrain properties and human features are relatively static in time and space. *Can the weather* – as a dynamic, short term influence (daily changes in temperature, moisture and wind conditions) – *be included as a separate risk factor?.*

The individual risks will first be reported as separate maps, then combined into an overall indication of fire hazard. How to combine the individual factors (weightings) is to be determined as the research progresses, and it thereby forms the final research question.

1.3 REPORT STRUCTURE

The following chapters describe:

- The study area (Ch. 2);
- The methods used (Ch. 3);
- The results (Ch. 4);
- Discussion (Ch. 5);
- Conclusions (Ch. 6).

2 STUDY AREA

The study area, of approximately 24 km^2, is situated in the La Peyne catchment, Hérault department, Languedoc-Roussillon, Southern France. It covers the surroundings of an artificial lake, Le barrage des Olivettes, near the village of Vailhan. The study area is trapezoid in shape (Appendix E), as a result of the north-west to south-east flight orientation of the HyMap satellite. The south-western and north-eastern borders are formed by the data extent of the flight line. The northwestern border is the straight line between the villages Pézenes-les-Mines and Valmascle. The southeastern border of the study area is formed by the powerlines going past the town of Neffiès.

The study area has a sub-Mediterranean climate with hot and dry summers and relative cool winters. Daily temperatures vary from an average 11˚C in January to 30˚C on average in July. Precipitation falls during spring and mainly autumn, with high intensities. The annual precipitation is 600 mm on average, but highly irregular over the years and is by far exceeded by the yearly potential evapotranspiration of almost 1100 mm, which is calculated using the Penman methods. The number of days with precipitation vary between 70 and 80 days per year and the amount of sunshine is 2700 hours per year (Sluiter, 2005).

Altitudes in the study area vary from 480 meters in the northern part to 105 meters in the south-eastern part. The steepest slopes can be found in the Peyne river valley and around the artificial lake. The south-eastern part is characterized by more gentle slopes and plains.

The Peyne river flows from north-west to south-east through the study area and is a contributor to the Hérault River. It is characterized by an irregular discharge regime. Highest discharges occur during spring whereas during summer most rivers have only little or no discharge. The artificial lake, Lac des Olivettes, was constructed to prevent flooding during hazardous rainfall events and for irrigation, and comprises a surface of around 40 hectares.

In the Peyne area, most of the natural vegetation can be separated into three classes; (i) the shrubby degraded evergreen forests called *maquis*, (ii) smaller shrubs and bushes called *garrigue* and (iii) grasses, herbs and very short bushes called *landes* (Tomaselli, 1981). The maquis is dominated by the *Quercus ilex* and *Arbutus unedo*.

The land cover of the study area is dominated by forests and garrigue vegetation. Some agricultural lands can be found in the southern part. The areas with garrigue and lands vegetation are sometimes used for herd grazing. The northern part of the catchment, around the lake, is dominated by dense *Quercus Ilex* forests. In the north eastern corner, unlogged parts of the forest contain *Quercus, Castanea* and *Buxus* trees.

Fire, both natural and human-caused, has played a large part in shaping the ecology of Mediterranean eco-regions. Hot, dry summers make much of the region prone to fires, and lightning frequently causes fires in the summer. Many of the plants are pyrophytes (fire-loving), adapted or even depending on fire for reproduction, recycling of nutrients, and the removal of dead or dying vegetation.

As for fire hazard, by far the highest natural risk is found in the maquis type of vegetation: these often dense, previously logged forests contain a high amount of small stems, and high volumes of (woody) fuel between the canopy and the ground. Compared to the broader, thicker stems of the older trees in unlogged areas, the small stems in the maquis forests result in a much greater surface area for a fire to “grab on to”, and they thus pose a much greater risk of a fire to grow and quickly spread out. Garrigue and landes areas are associated with a lower fire risk, due to their lower connectivity: they contain open, bare ground, hindering the spread of a fire.

Fire hazard associated with agricultural lands varies according to their state of use: active plots will have a high moisture content due to irrigation, and therefore are of lesser concern than abandoned plots, which may contain large numbers of dead, dried out crops. During long periods of draught, vineyards may pose an increased risk, as irrigation on these plots is not allowed. Machinery, used on active plots, can increase the risk of ignition of the surrounding vegetation. To restore nutrient levels in the soil, abandoned plots are sometimes deliberately burned down; a process that could get out of control and spread to neighboring vegetation.

The Peyne area is situated within the transition zone of four major geological zones; the metamorphic rock plateaux of the Massif Central in the north and the Montagne Noir in the west, the alluvial sediments of the Hérault river in the east, and the coastal plain in the south to southeastern part of the area. The Montagne Noir is part of the continental water divide: streams and rivers on the west and north slopes lead towards the Atlantic Ocean, while on the south and east side (including the Peyne) they end up in the Mediterranean Sea. Rock types found in the area include limestone plateaus, sandstone and dolomite formations, and volcanic tuffs and basalt outflows (Géze, 1979).

3 METHODS

After a brief overview of existing modeling systems for wildfires (§3.1), the methods used to answer each of the five research questions are described:

- Mapping vegetation risk (§3.2);
- Mapping human risk (§3.3);
- Mapping topographic risk (§3.4);
- Mapping weather risk (§3.5);
- Creating the combined, overall hazard map (§3.6).

3.1 MODELLING WILDFIRE HAZARD & BEHAVIOR

3.1.1 ROTHERMEL MODEL

Rothermel (1972) developed a deterministic, dynamic spatial fire model for wildland fuels. Unlike previous models that required inputs that could not readily be determined before combustion occurred, the Rothermel model predicts fire behavior (spread rate and intensity) from three types of parameters:

- parameters describing fuel availability
  (e.g. fuel loads and packing ratios);
- parameters describing the conditions under which the fire burns (time- & space-dependent)
  (e.g. fuel moisture, proportion of live and dead fuels, wind velocity, slope steepness);
- parameters describing a fuel's physical properties
  (e.g. mineral content, low heat of combustion, average surface area to volume ratio).

A limitation of the Rothermel model is that it assumes a steady-state rate of spread, and that fuels are uniform and continuous, both in horizontal and vertical direction (Kessell *et al.*, 1978). These uniformity assumptions are most often violated by naturally occuring fuel compositions.

3.1.2 FUEL CHARACTERISTIC CLASSIFICATION SYSTEM

The Fuel Characteristic Classification System (FCCS), proposed by Ottmar *et al.* (2007), contains a set of over 200 fuelbeds representative for the United States. They were compiled from scientific literature, fuels photo series, fuels data sets, and expert opinion. The system enables modification and enhancement of these fuelbeds to represent a particular scale of interest. The FCCS then reports assigned and calculated fuel characteristics for each existing fuelbed stratum including the canopy, shrubs, non-woody, woody, litter–lichen–moss, and duff. Finally, the system classifies each fuelbed by calculating fire potentials (Figure 3.1).

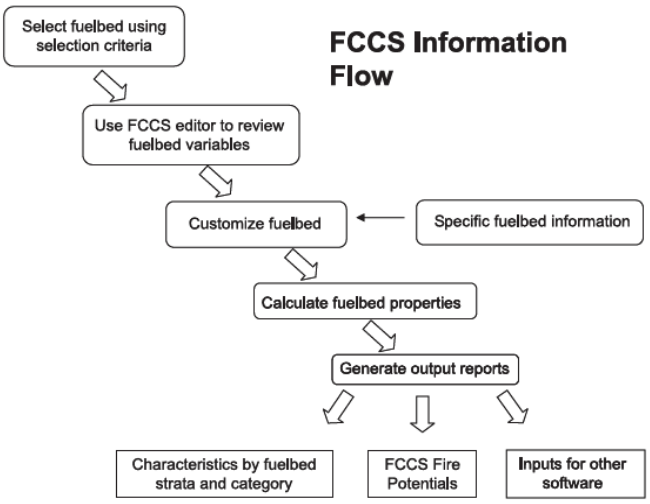

FIGURE 3.1 – FCCS (FUEL CHARACTERISTIC CLASSIFICATION SYSTEM) FLOW CHART. (TAKEN FROM: OTTMAR ET AL., 2007)

The FCCS stratifies fuelbeds into six horizontal strata (figure 3.2; 3.3), in order to represent every fuel element that has the potential to combust and to better assess potential fire effects from each combustion phase of a fire. Each fuelbed stratum is separated into one or more fuelbed categories, with a further division into subcategories, allowing for addition or exclusion of as much detail as desired. The fully characterized fuels are then used to compute the fuelbed's specific FCCS fire potentials (figure 3.4) (Riccardi *et al.*, 2007a); intended for use in mapping fire hazard, categorizing fuelbeds on the basis of predicted fire behaviour, predicting and measuring the effects of fuel treatment, and to ease communication of the degree of hazard (McKenzie *et al.*, 2007; Ottmar *et al.*, 2007; Sandberg *et al.*, 2007a; Sandberg *et al.*, 2007b; Schaaf *et al.*, 2007). The fire behaviour potentials are based on a reformulation of the aforementioned Rothermel model.

FIGURE 3.2 – STRATIFICATION OF THE FCCS FUELBEDS (FROM: OTTMAR ET AL., 2007).

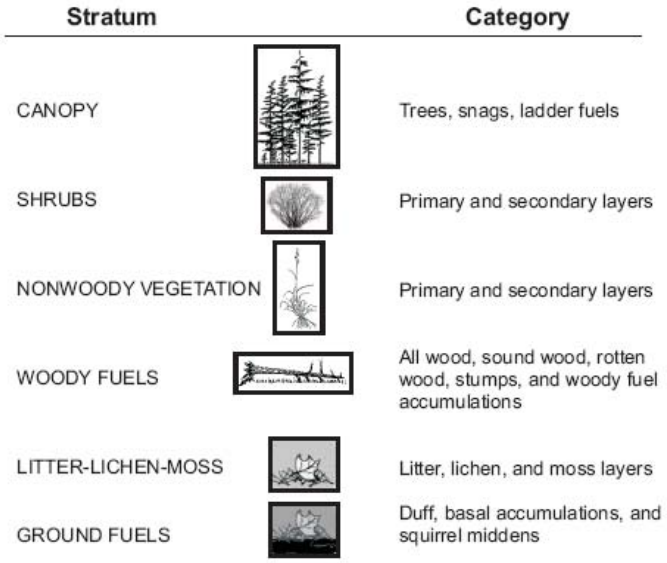

FIGURE 3.3 – STRATIFICATION OF THE FCCS FUELBEDS (FROM: OTTMAR ET AL., 2007).

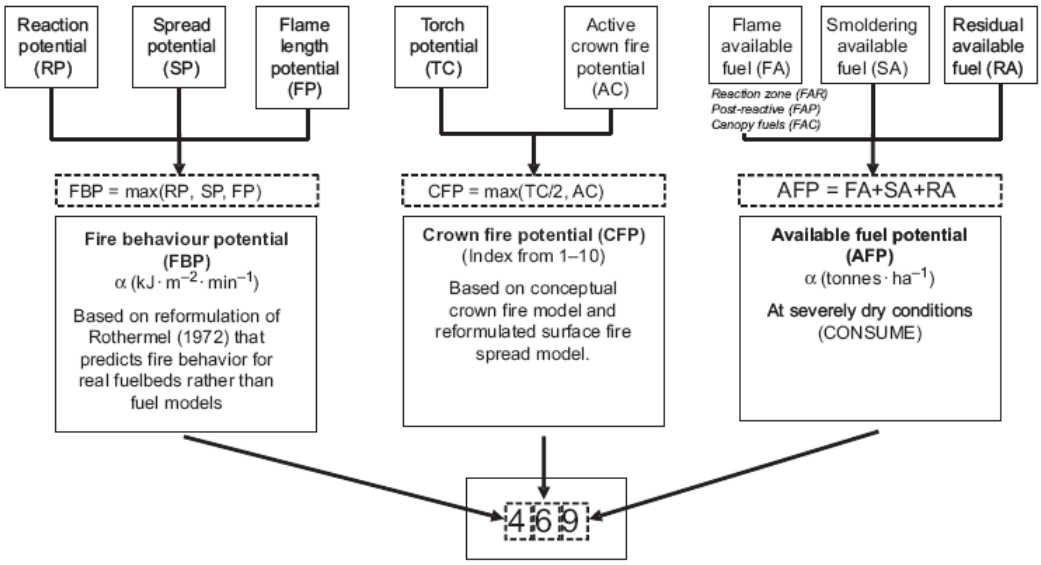

FIGURE 3.4 – FCCS FIRE POTENTIALS AND THEIR RESPECTIVE COMPONENTS (TAKEN FROM: SANDBERG ET AL., 2007B)

The FCCS accommodates a wide range of potential users, operating at various scales and with different levels of detail, data quality and data quantity. Data and methods were considered scientifically credible by participants of several regional workshops given to land managers, scientists and policy makers (Ottmar *et al.*, 2007). Its outputs incorporate natural fuelbed variability, are standardized and repeatable (Riccardi *et al.*,2007b). They are currently being used in a national wildland fire emissions inventory and in the development of fuelbed, fire hazard, and treatment effectiveness maps on several national forests (McKenzie *et al.*, 2007).

The FCCS – and nearly all other modeling techniques based on Rothermel's spread model - were built for the United States, and as such they usually concern very specific, even locally occurring fuel types. However, the conceptual framework of the FCCS would be applicable worldwide (Ottmar *et al.*, 2007) because of high flexibility and potential for expansion. The original 13 (Anderson, 1982, after: Albini, 1978), along with the additional 43 fuel models (Scott & Burgan, 2005) for the Rothermel model will continue to be useful to fire managers using the current generation of fire behavior models.

ADAPTABILITY OF THE FCCS

While the literature states that the FCCS can be adapted to function worldwide (Ottmar *et al.*, 2007), personal exploration of the model's workings showed no possibility to adequately describe the local Mediterranean vegetation communities. Since the vegetation's properties do play a significant role in determining the final fire potentials (tried and tested during research preparation), it would be preferred to be able to incorporate it. To this end, a system with a European base was found (§3.1.3).

3.1.3 PROMETHEUS FUEL CLASSIFICATION SYSTEM

European researchers developed a new fuel type classification system that is better adapted to fuels found in European Mediterranean ecosystems (Riaño *et al.*, 2002). It was constructed within the Canadian Prometheus project's framework, as used by the Canadian Interagency Forest Fire Centre (CIFFC). Similar to the Rothermel fuel models, the Prometheus fuel types were defined for surface fire modeling, based on type and height of the fire propagation element. Seven fuel types are distinguished (Figure 3.5; Riaño *et al.*, 2002):

1) **Ground fuels** (grass cover > 60%);
   Grasslands: agricultural and herbaceous vegetation.

2) **Surface fuels** (shrub cover > 60%, tree cover < 50%);
   Grasslands: low-lying shrubs (30-60 cm), high percentage (30-40 %) of herbs. Clear-cuts with slash not removed.

3) **Medium-height shrubs** (shrub cover > 60%, tree cover < 50%);
   Medium to large sized shrubs (0.6-2.0 m), young trees (regeneration and/or reforestation).

4) **Tall shrubs** (shrub cover > 60%, tree cover < 50%);
   Tall shrubs (2.0-4.0 m) and regenerating trees.

5) **Forest areas, no understory** (shrub cover < 30%, tree cover > 50%);
   Tree stands (> 4 m), includes areas where ground fuel was removed (prescribed burning or mechanical means).

6) **Forest areas, medium understory** (shrub cover > 30%, tree cover > 50%);
   Tree stands (> 4 m), distance between canopy base and surface fuel > 0.5 m. Small shrubs, grass, litter and duff.

7) **Forest areas, heavy understory** (shrub cover > 30%, tree cover > 50%).
   Tree stands (> 4 m), distance between canopy base and surface fuel <0.5 m. High and dense understory.

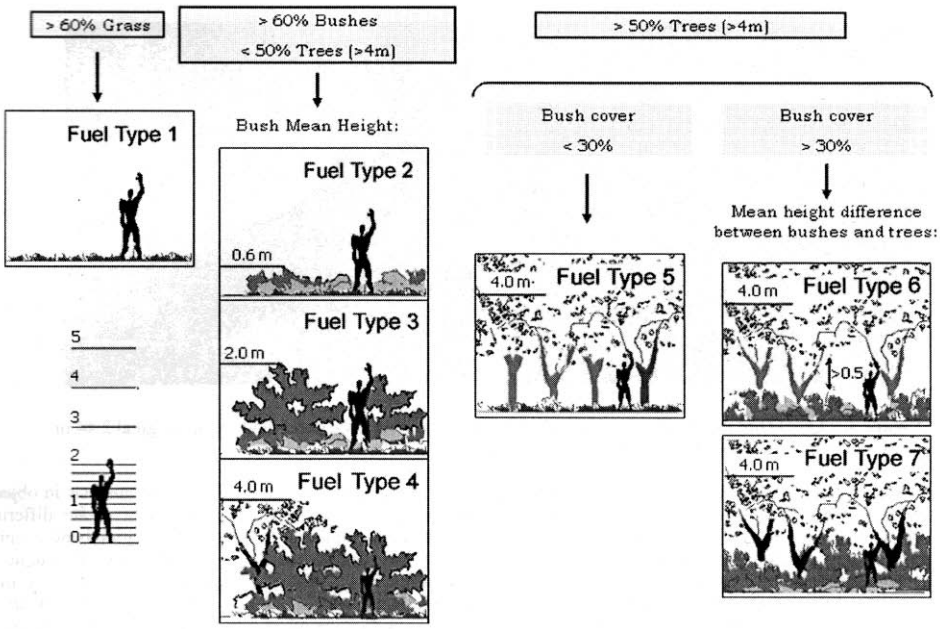

FIGURE 3.5 – PROMETHEUS FUEL CLASSIFICATION SYSTEM FOR MEDITERRANEAN SYSTEMS. OVERVIEW OF FUEL TYPES AND SELECTION CRITERIA (TAKEN FROM ARROYO ET AL., 2006)

3.2 VEGETATION RISK

3.2.1 COLLECTION OF FIELD DATA

In September and October 2009 a field campaign was organized, aimed at collecting the necessary field data. The planned plot locations (App. D) were selected based on:

- land use features derived from the topographic map (Appendix A);
  (e.g. isolated forest stands, exclusion of villages and agricultural areas);
- slope and/or elevation (from the DEM) (Appendix B);
- patterns in NDVI values (Appendix C).
  (constructed from HyMap 2008 data);

Areas with accessibility limitations (no roads/tracks), were left unsampled. Agricultural areas were not considered for fuel type mapping, because of their relatively high maintained moisture content, but also because of their very temporal character (short lifespan of contained crops). After recording the general properties of a plot, measurements and observations were divided across the 6 different strata contained within the FCCS (figure 3.3)

Recordings took place on the field form (App. F). It contains sections for each of the strata, not all of which were required for every plot location; should one of the strata, or a part there in, be absent it could be skipped on the form. Measurements on moisture content and canopy coverage calculated from hemispherical photographs were carried out and added to the form at the end of each field day. Each plot form was then digitalized for further analysis at Utrecht University.

GENERAL PLOT PROPERTIES

The precise coordinates of the plots were determined from the digital, geo-referenced map and then located in the field using a GPS. In cases where the planned location was inaccessible, an alternative location was selected based on the same maps used in the preparation phase (appendices A-C). The aim was to keep the plot within the same map units / vegetation stand, for as much as possible.

Appendix E depicts the actual plot locations. To reduce the effect of weather trends during the two month field period, the plots were not measured in a spatial sequence but in smaller subseries, randomly done across the length of the field campaign.

At the start of plot sampling, it was assigned one out of the seven possible Prometheus fuel types; their selection criteria are shown in figure 3.5. The plot sized used was 3x3 m. If needed in later calculations, absolute quantities per plot (e.g. number of trees, number of woody elements) would be multiplied by 2.77 (25 m^2 / 9 m^2) to acquire a quantity that is representative of a single HyMap image pixel (5x5 m).

COVER

Canopy coverage (%) was estimated by visual observation, as well as with a hemispherical camera, equipped with a *fisheye* lens. Four to five photographs (depending on the size of the tree) were taken surrounding the base of the tree under consideration, facing upwards. The accompanying software (CanEYE) produces values for cover fraction and LAI (Leaf Area Index) by classifying the digital photograph's pixels into air (white/blue) and vegetation (green/brown). Cover percentages for the other FCCS strata (figure 3.3), such as shrubs and litter, were only estimated by eye.

MOISTURE CONTENT

To be able to compare patterns in the (canopy) moisture content with patterns derived from the HyMap images, destructive samples were taken from the canopy of each plot. If there was no canopy present, the shrub layer was sampled instead. Because it's the topmost layer of vegetation in that case, It will also show up on the HyMap images. Besides the canopy, the litter layer was sampled to determine its moisture content. The samples were weighed, dried in an oven at 104°C for 15 hours (Roberts *et al.*, 2006), then reweighed to determine live fuel moisture content:

$$LFM = (W_w - W_d)/(W_d) * 100 \quad (1)$$

with: LFM = Fuel Moisture (%)
W_w = wet weight (g)
W_d = dry weight (g)

Heights, diameters and depths of the different strata were determined with measuring tools such as a ruler, tape measures and measuring rods. DBH (Diameter at Breast Height) was measured as CBH (Circumference at Breast Height), then transformed to DBH in the computer by dividing CBH by π.

To measure the required parameters for the woody fuel stratum, two 3 m transects were placed in the plot. One cross-slope, one up-slope, so that they formed two perpendicular boundaries of the plot, with their origin being the location depicted on the plot location map. Along each transect, the amount of woody particles (twigs, parts of branches), that crossed the transects was recorded (Brown, 1974) per size-class (table 3.1). By multiplying the amount of elements on the upslope transect by the amount of elements on the cross-slope transect, an estimate can be retrieved for the total amount of elements in the entire plot.

To estimate the loadings (kg) of the woody fuel stratum, three elements from the most abundant size class encountered within the plot were destructively sampled: the element nearest to the origin (E_o), the element nearest to the end of the upslope transect (E_u), and the element nearest to the end of the cross-slope transect (E_c).

Woody	cover (%)	depth (cm)

Sample	Class most abundant	Total (g)	Dried (g)	Avg. Weight /element (g)
	-			
	3 elements: nearest to origin & transect ends			

Sound (cm)	# / upslope transect	# / crossslope transect	Species
0 - 0.64			
0.64 - 2.54			
2.54 - 7.62			
7.62 - 22.86			
22.86 - 50.8			
> 50.8			
Rotten (cm)	**# / upslope transect**	**# / crossslope transect**	**Species**
7.62 - 22.86			
22.86 - 50.8			
> 50.8			

TABLE 3.1 – APPENDIX F – SECTION "WOODY"

To obtain an estimate of the average weight per element, the samples were dried to remove all moisture, similar to the determination of LFM. The total W_d was then divided by 3 to get an estimate of the average weight per element in the plot. The total woody fuel loading is then:

$$WFL = T_u * T_c * \frac{W_d}{3} \quad (2)$$

with: WFL = Woody fuel loading of the plot (kg)
T_u = amount of elements of all sizes crossing the upslope transect
T_u = amount of elements of all sizes crossing the cross-slope transect
W_d = combined dry weight of E_0, E_u, E_c (kg)

3.2.2 IMAGE ANALYSIS

To produce a risk map based on vegetation, the study area was classified according to the observed Prometheus fuel types (figure 3.5). To this end, two supervised classification methods were compared: the Minimum Distance to Mean and the Maximum Likelihood classifier. Water and No Vegetation/ Agricultural classes were defined by selecting training areas in the middle of the lake, a vineyard in the southeastern part of the study area, a clear road and parking lot near the lake and a building in the village of Vailhan.

The maximum likelihood classification method is based on the assumption that the occurring values are normally distributed within each category (Lillesand *et al.*, 2004). Applied to the Prometheus fuel types this means that it is assumed that the values in each of the HyMap-image's bands, are normally distributed within each of the seven fuel types. Using the sample mean and covariances, a response pattern is determined for each fuel type, across all reflectance bands. The statistical probability is then calculated of a pixel being a member of a certain class; the pixel is eventually assigned to the class to which it is most likely to belong.

In contrast to the maximum likelihood method, the minimum distance to mean classifier does not include (co)variance; it assigns a class to an unknown pixel only on the basis of the nearest class mean, across all included reflectance bands. Because it uses the sample mean, not the population mean, to calculate a covariance matrix for each reflectance band, the maximum likelihood classifier needs more sample points than reflectance data bands (number of bands + 1) in order to compute all the needed statistics per fuel type to be assigned. Should the number of occurrences for a given Prometheus fuel type be insufficient to include all 126 existing reflectance bands in the HyMap image, either it needs to be omitted from further analysis, or the number of bands needs to be reduced to match the number of observations. This data reduction can be achieved by means of a Principal Component Analysis (PCA).

Principal Component Analysis is designed to reduce data redundancy in multispectral data. In short: its purpose is to compress all of the information contained in an original *n*-band data set into fewer than *n* new bands (Lillesand *et al.*, 2004). It is used to increase the computational efficiency and/or data storage requirements of the dataset. PCA redefines the directions of the axes describing the data; the first principal component (1st new axis) contains the largest percentage of total scene variance. Each succeeding principal component contains a decreasing percentage of the scene variance, and is always orthogonal to all previous principal components, ensuring the data they contain are uncorrelated. Applied to the maximum likelihood classifier used for the Prometheus types in this research, PCA can be used to reduce the number of data bands to the maximum allowed

amount (number of observations – 1), while still retaining as much scene variance as possible. Out of the two classifiers, the one that yields the best result (based on accuracy and agreement with field experience) will be used to create the basis for the vegetation risk map.

3.2.3 VEGETATION RISK ASSESSMENT

After classification, each encountered Prometheus type (§2.3.3) was assigned a risk value based on vegetation. To compute these values, six of the recorded field parameters (appendix F) were used:

- primary shrub cover (%);
- secondary shrub cover (%);
- amount of dead primary shrubs (%);
- amount of dead secondary shrubs (%);
- woody fuel cover (%);
- litter coverage (%).

Each of these parameters was assigned a risk value between 0 and 4, based on its value (table 3.2). At 100% cover, the parameter's risk value is at its maximum; at 0% cover, the parameter's risk value is at its minimum. If 100% of the vegetation (canopy, shrubs, non woody) is alive, the parameter's risk value is at its minimum; if 0% of the vegetation is alive (i.e. 100% of the cover is dead material), the parameter's risk value is at its maximum. Averaging the risk values of all 6 parameters yielded a vegetation risk value for a particular plot.

	Shrub Cover (%)		**% alive**		**Woody**	**Litter**
	primary	**secondary**	**primary**	**secondary**	**cover (%)**	**cover (%)**
Maximum risk **(4)**	100	100	0	0	100	100
Minimum risk **(0)**	0	0	100	100	0	0

TABLE 3.2 - DETERMINATION OF VEGETATION PARAMETER RISK VALUES. FOR EACH PARAMETER, THE PARAMETER VALUE ASSOCIATED WITH THE MAXIMUM RISK VALUE (4) AND MINIMUM RISK VALUE (0) IS GIVEN. BETWEEN MINIMUM AND MAXIMUM PARAMETER VALUES, THE ASSOCIATED RISK VALUE IS LINEARLY DISTRIBUTED.

For each Prometheus type encountered in the study area, the risk values for all plots contained within it were then combined to retrieve the average risk value associated with that Prometheus fuel type. This process is shown schematically in figure 3.6. This indirect approach was taken as some of the parameters (mostly woody and litter cover) would not be visible – and thus classifiable – from the remotely sensed imagery.

The final map of vegetation risk per Prometheus type was created by ranking the encountered Prometheus types according to their calculated risk value: class 1 for the Prometheus type with the lowest risk value, and class 4 for the one with the highest risk value. The other occurring Prometheus types were assigned classes in between those two extremes, at equal intervals. Locations with no vegetation (parking lots, houses, water) were assigned no risk (class 0).

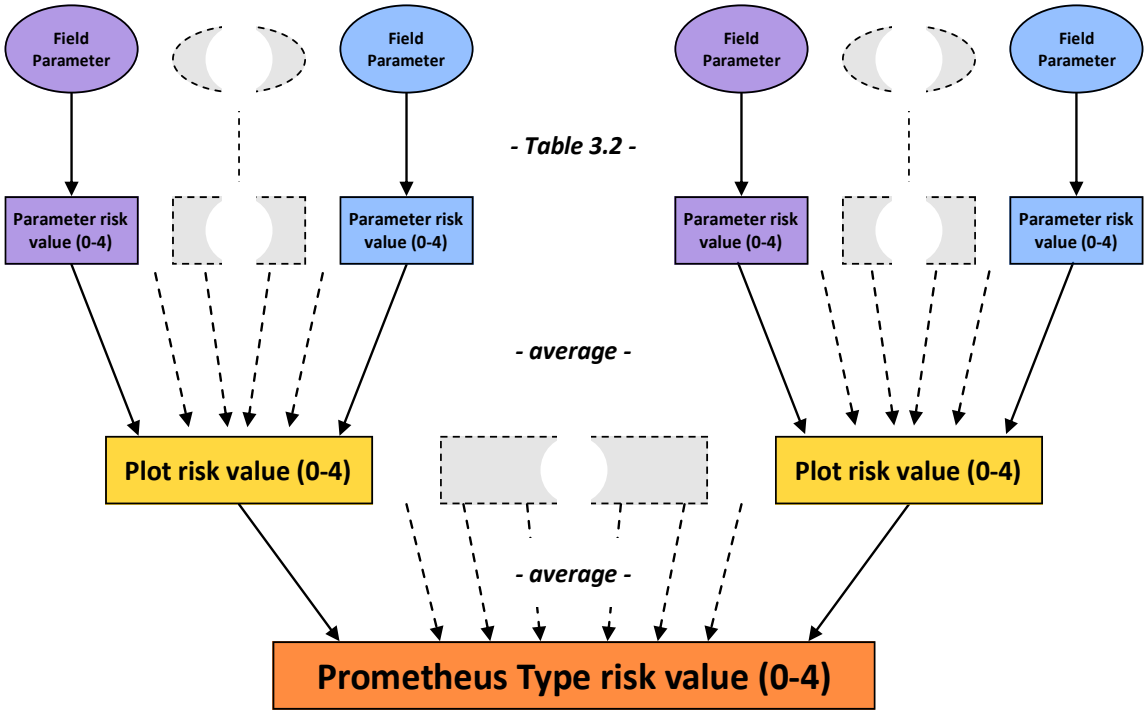

FIGURE 3.6 – FLOWCHART DEPICTING THE ASSIGNMENT OF RISK VALUES TO A PROMETHEUS TYPE, BASED ON FCCS PARAMETERS MEASURED IN THE FIELD.

3.3 HUMAN RISK

To classify manmade structures, the original HyMap image was classified using a supervised minimum distance to mean classifier. Training areas ("ground truth" references) were used to distinguish between three major land use types: water, natural vegetation and manmade structures (e.g. roads, buildings). To be able to exclude as much vegetation as possible from the classification process, so as to avoid potential influence from areas that are fully vegetated, an NDVI-image was computed out of band 14 (red, 486 nm wavelength) and band 39 (near-infrared, 1004 nm wavelength) of the HyMap2008 imagery:

$$NDVI = \frac{NIR - RED}{NIR + RED} \tag{3}$$

All image pixels with an NDVI value above 0.5 were then masked out in the classification calculations: setting this to a lower value lower would result in exclusion of the desired features, i.e. pixels known to be part of a road or building would be excluded due to their reflectance mixing with that of neighboring or interfering objects (overhanging vegetation, grid cell containing more than one type of feature class).

To create the human risk map, buffer zones of 25 meters were then mapped around features such as villages, houses, farms, power lines, roads and (hiking)trails, to indicate the increased possibility of ignition due to human activity (§2.2.4). The edges of the structures were assigned the highest risk

(class 4), while everything at a distance greater than 25 meters was assigned no risk (class 0). The manmade structures and agricultural areas themselves receive no additional risk value. Asphalt or sand does not burn; (alive) agricultural crops are artificially kept at a high moisture content and, especially in the case of vineyards, the spacing of individual plants/shrubs is much more open. Both risk of ignition and fire spread rate are thus limited in these areas.

3.4 TOPOGRAPHIC RISK

From the DEM of the study area, topographic risks were assessed (slope steepness, aspect). A risk value based on slope was derived from a formula used by Rothermel (1972), determining a slope factor that increases surface fire spread rate:

$$\phi_s = 5.3 \cdot \tan^2(\alpha) \cdot \beta^{-0.3} \qquad (4)$$

with: ϕ_s = slope factor (-)
α = slope (degrees)
β = packing ratio of fuel particles (-)

The packing ratio is a measure of fuelbed compactness, i.e. the fraction of the fuel volume that is occupied by fuel (Rothermel, 1972 in: Riccardi *et al.*, 2007B). At very low packing ratios, fire spread is limited and fire intensities are low. At very high packing ratios, the lack of oxygen limits fuel combustion. In order to obtain a risk value solely based on slope steepness, the packing ratio of fuel particles (which did not belong to the parameters recorded during the fieldwork) was assumed equal for the entire study area. As a result, this term could be eliminated from equation 3.

A slope of 45 degrees was the maximum slope encountered on the DEM of the study area and its resulting slope factor was therefore associated with the highest risk value (4). All other slope factors would therefore be arranged on a continuous scale between 0 and 4, as is shown in figure 3.7.

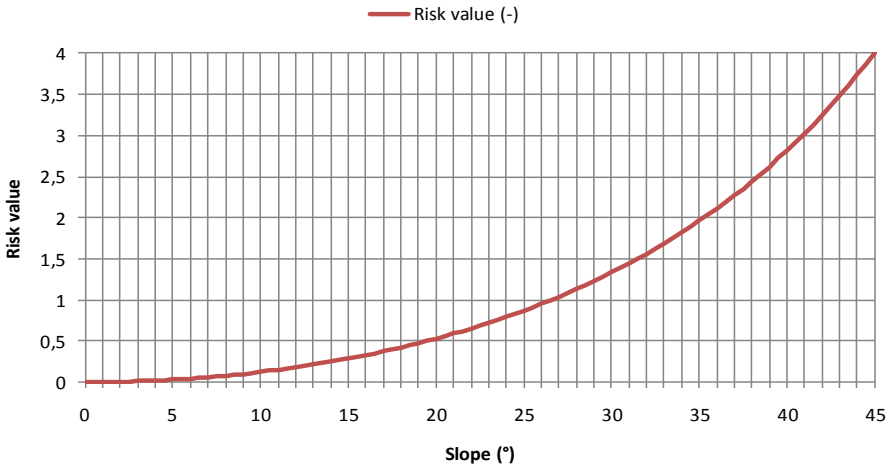

FIGURE 3.7 – GRAPHICAL REPRESENTATION OF EQUATION 3: CALCULATING SLOPE (RISK) FACTOR FROM SLOPE STEEPNESS

Aspect risk (§1.1.2) is determined by calculating slope aspect values (0-360°) from the DEM. They are then assigned risk values on a continuous scale between 0 and 4, as is depicted in figure 3.8. The highest risk value is assigned to south facing slopes (180°), which receive the most intense and longest period of direct sunlight. The lowest value, 0, is assigned to north facing slopes (0°) as they receive no direct sunlight at all. As numerical intermediates, east and west facing slopes are assigned a risk value of 2.

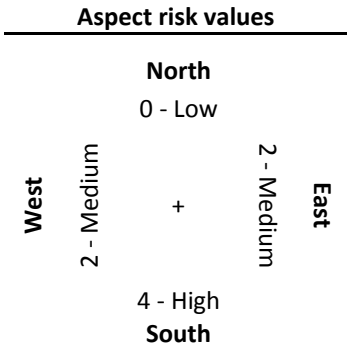

FIGURE 3.8 – SLOPE ASPECTS ARE ASSIGNED CONTINUOUS RISK VALUES FROM 0 (NORTH) TO 4 (SOUTH) AND BACK TO 0 (NORTH) AGAIN

3.5 COMBINED FIRE HAZARD

While each of the maps described in this section (vegetation risk, human risk, and topographic risk) can individually and independently show specific types of (relative) fire hazard, the most interesting course of action is to combine them into one map.

The maps mentioned above all have their risk values set to be between 0 and 4, indicating the minimum and maximum risk class. In combining the individual maps, weight factors are applied to the summation of their risk values, so as to balance the influence each of the risks has on the final, overall fire hazard. Three combinations of weights were used:

- **1x Vegetation risk value + 1x Human risk value + 1x Topographic risk value**
  Used as a control; initial state with all factors of equal influence.

- **1x Vegetation risk value + $^{2}/_{3}$ x Human risk value + $^{1}/_{3}$ x Topographic risk value**
  Both the FCCS and Prometheus modeling systems rely heavily (if not only) on vegetation properties. As such, this is kept as strongest contributor to the overall fire hazard. Human risk is the most prominent in the start of wildfires, and it is therefore given a stronger contribution than risk caused by a location's topography. The relative difference between the three factors was chosen arbitrarily; the absolute difference was kept constant ($^{1}/_{3}$).

- **1x Vegetation risk value + $^{3}/_{5}$ x Human risk value + $^{1}/_{5}$ x Topographic risk value**
  This alternative combination, with the same order of influence and a constant – but greater – absolute difference ($^{2}/_{5}$), was used to see whether or not slight changes in weight factors would be visible in the resulting hazard map.

4 RESULTS

4.1 VEGETATION RISK MAP

4.1.1 FIELD MEASUREMENTS AND OBSERVATIONS

PLOT LOCATIONS

During the fieldwork, the planned plot locations (appendix D) were approached by using a handheld GPS system. Due to its inaccuracy of a few meters, varying with weather and overhead vegetation conditions, the actual plot locations differ from the planned locations. Figure 4.1 shows the difference in meters between the planned and actual plot locations.

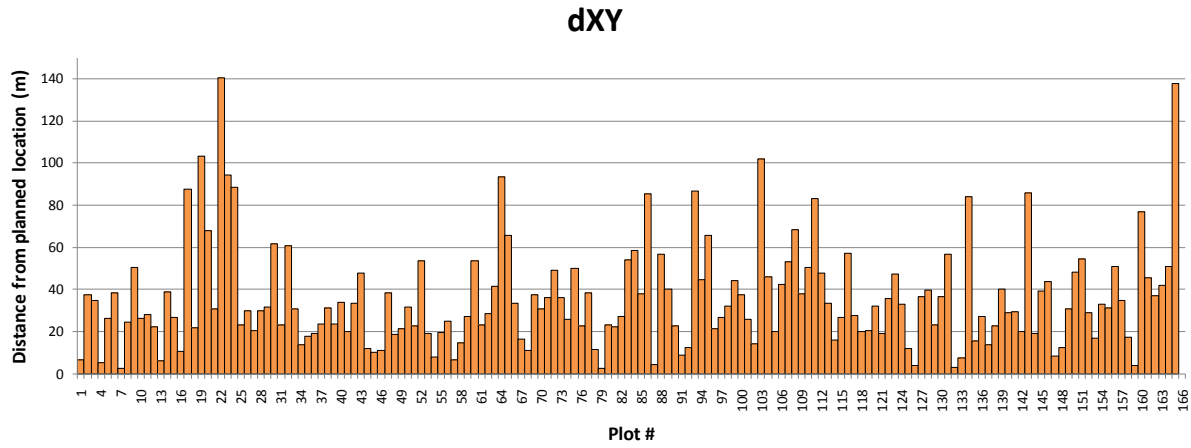

FIGURE 4.1 – DIFFERENCE BETWEEN PLANNED AND ACTUAL PLOT LOCATIONS

OBSERVED PROMETHEUS TYPES

For each of the seven Prometheus types (§3.1.3), figure 4.2 shows the number of plots it was encountered in. Type 5 (<30% shrubs; >50% trees) was the most abundant; Type 1 (>60% grass) and Type 2 (>60% shrubs 0.3 – 0.6 m; <50% trees) were not encountered during the fieldwork. Type 7 (>30% shrubs, >50% trees; heavy understory) was only found on two occasions. Appendix H is a map showing the Prometheus type for each plot location. Type 3 is commonly found in the southern part of the study area, at the riverbanks and near the road on the east side of the lake. Plot 68 (along the x=525000 gridline) and its surroundings showed signs of recent logging; a likely explanation for the absence of trees (unexpected considering adjacent plots). Type 4 is found most in the western part of the study area. Type 6 was encountered in the north and eastern parts of the study area.

Number of plots per Prometheus Type	
Type 1	0
Type 2	0
Type 3	14
Type 4	42
Type 5	80
Type 6	28
Type 7	2

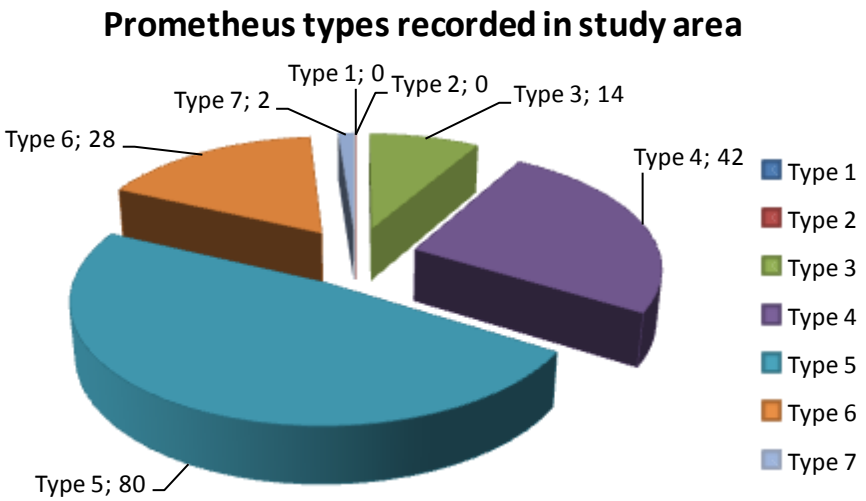

FIGURE 4.2 – OCCURRENCES OF DIFFERENT PROMETHEUS TYPES WITHIN THE STUDY AREA

COVER

Figure 4.3 shows the difference in cover fraction estimated by eye, and cover fraction determined by the CanEYE software. On average, the difference was -8%, i.e. the estimated cover fraction was 0.08 smaller than the calculated cover fraction. The most extreme differences occurred for plots in which the vegetation was relatively open; the photos taken from a single tree lead to a much higher cover percentage then the visual estimate, which also takes the surrounding vegetation into consideration. In case of plot nr. 57, the extreme positive difference (estimated cover fraction 0,65 higher than calculated), the opposite may be true: the individual tree was more open than the plot as a whole.

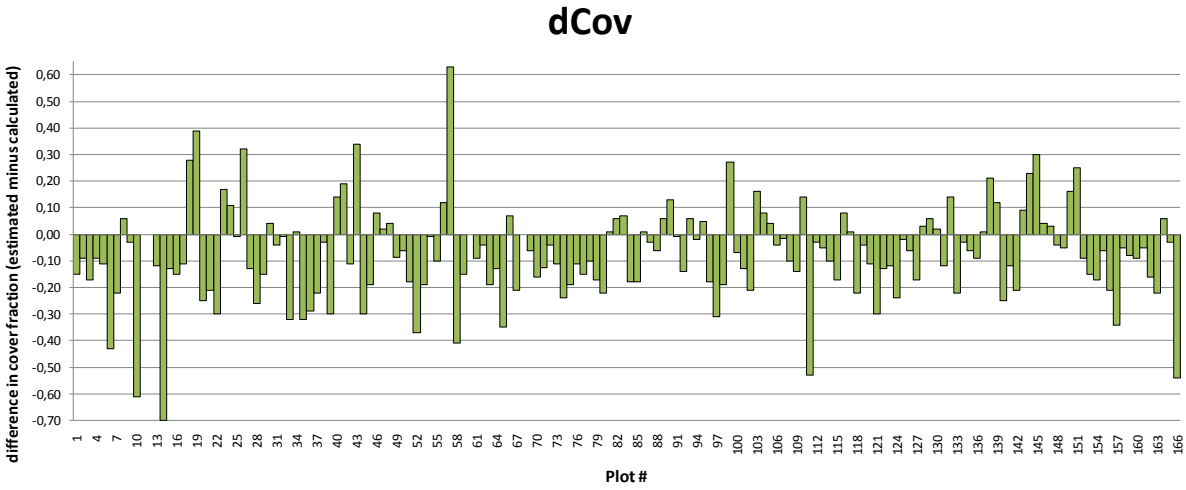

FIGURE 4.3 – DIFFERENCE BETWEEN COVER FRACTION AS ESTIMATED BY EYE, AND AS DETERMINED BY THE CANEYE SOFTWARE BY MEANS OF HEMISPHERICAL PHOTOGRAPHS

Figures 4.4 and 4.5 show the surface fuel (canopy and/or shrubs) cover per Prometheus type, based on the estimated cover fractions; the calculated cover fractions (hemispherical photographs) were considered to be too much of a point source compared to the estimated cover fraction of the entire plot. Since both parameters form the selection criteria in the Prometheus classification system, they follow its design: Type 3 has a lowest canopy, and highest shrub cover. Type 4 has a significantly higher shrub cover than types 5, 6 and 7. Type 5 has the lowest shrub cover. Type 5, 6 and 7 have similar canopy covers, although the min-max range of type 5 is much larger.

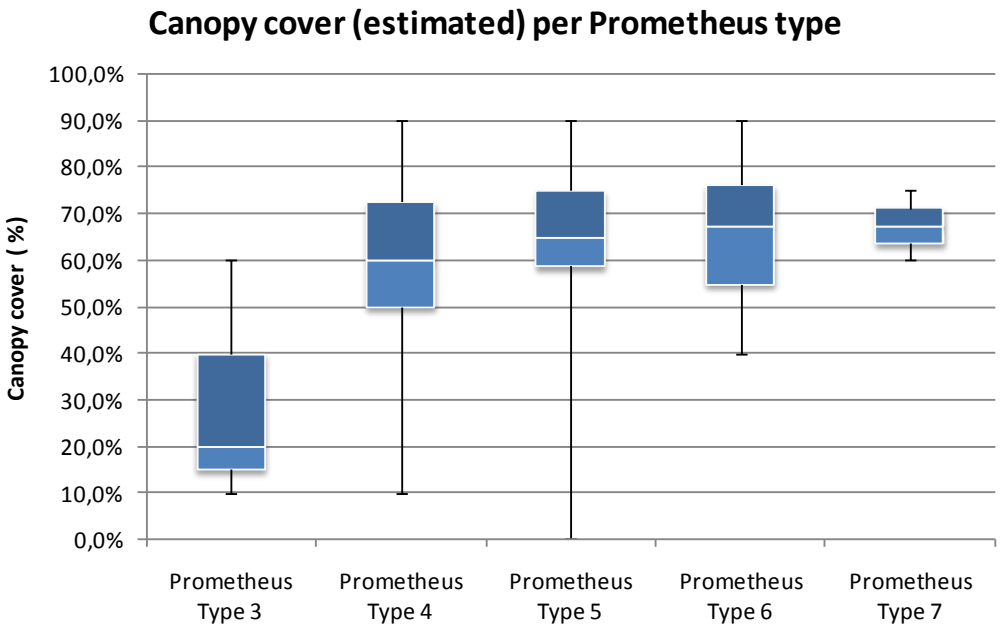

FIGURE 4.4 - BOX-WHISKER PLOT OF ESTIMATED CANOPY COVER PER PROMETHEUS TYPE

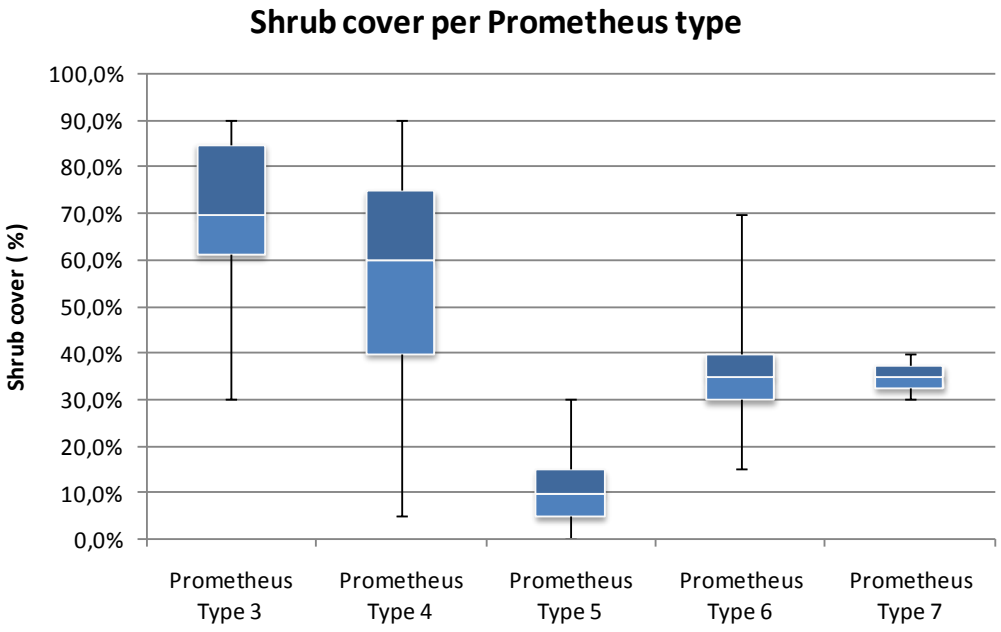

FIGURE 4.5 - BOX-WHISKER PLOT OF SHRUB COVER PER PROMETHEUS TYPE

Figures 4.6. and 4.7 show the ground fuel (woody and litter) cover per Prometheus type. On average, type 3 has the lowest amount of ground fuel, the other 4 types have very similar quantities. Type 6 has the highest woody fuel cover, type 5 the highest litter cover.

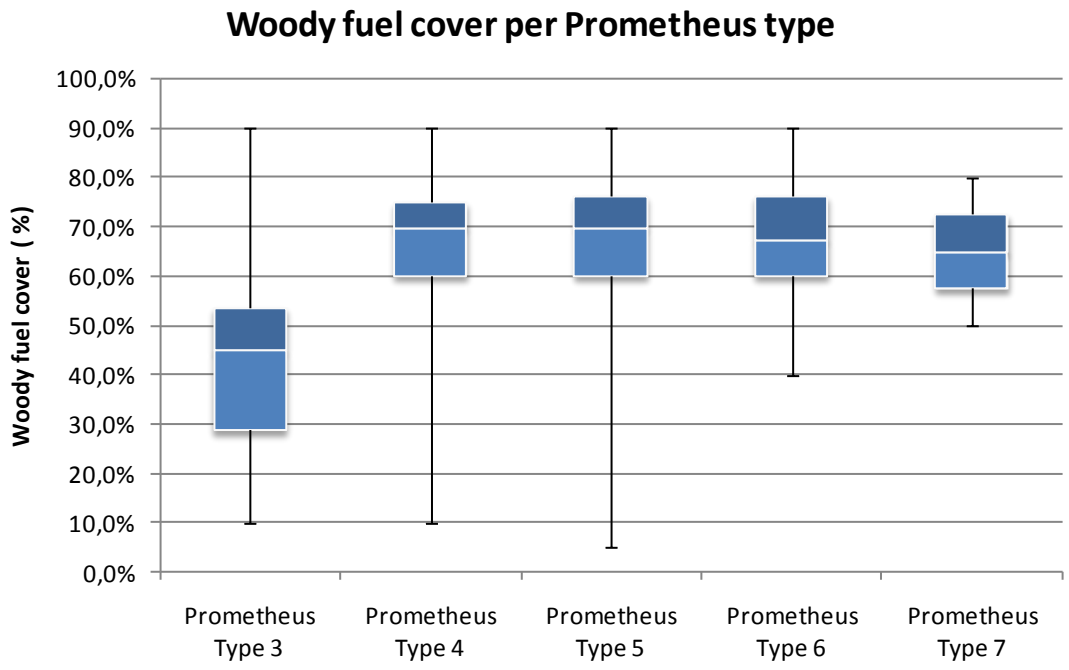

FIGURE 4.6 – BOX-WHISKER PLOT OF WOODY FUEL COVER PER PROMETHEUS TYPE

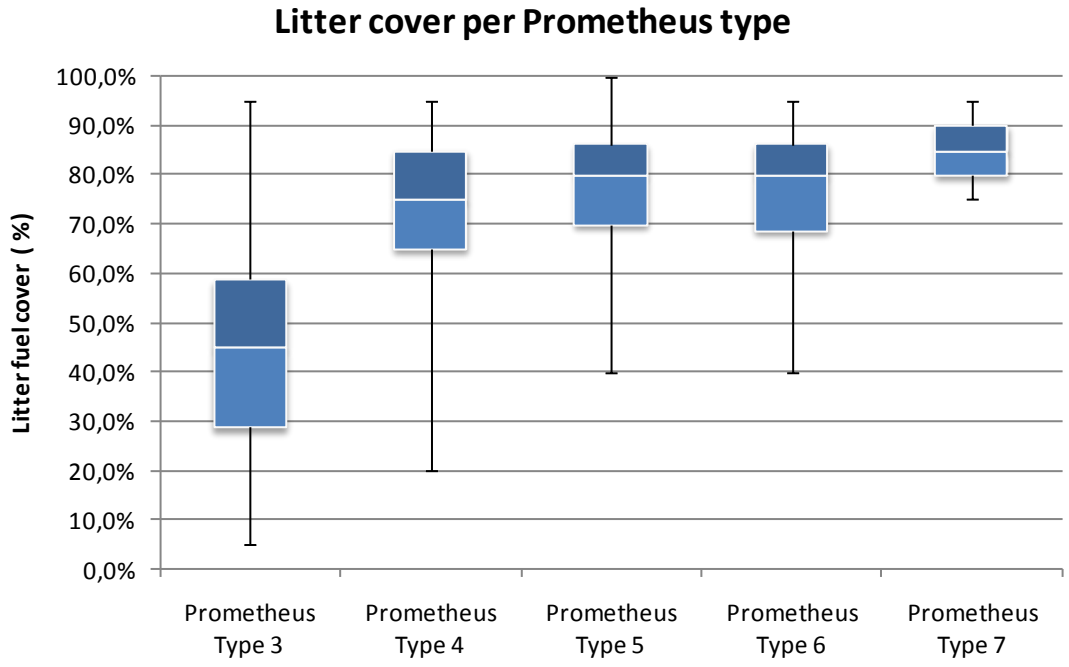

FIGURE 4.7 – BOX-WHISKER PLOT OF LITTER COVER PER PROMETHEUS TYPE

Figure 4.8 shows the canopy and litter moisture content per Prometheus type. While type 4 and type 5 have a broader range of measured moisture content than the other types; the average values of all types are close together: ranging from 43.9 % to 46.8%, for type 6 and 7 respectively. The moisture content of the litter samples slighty increases for the higher Prometheus types.

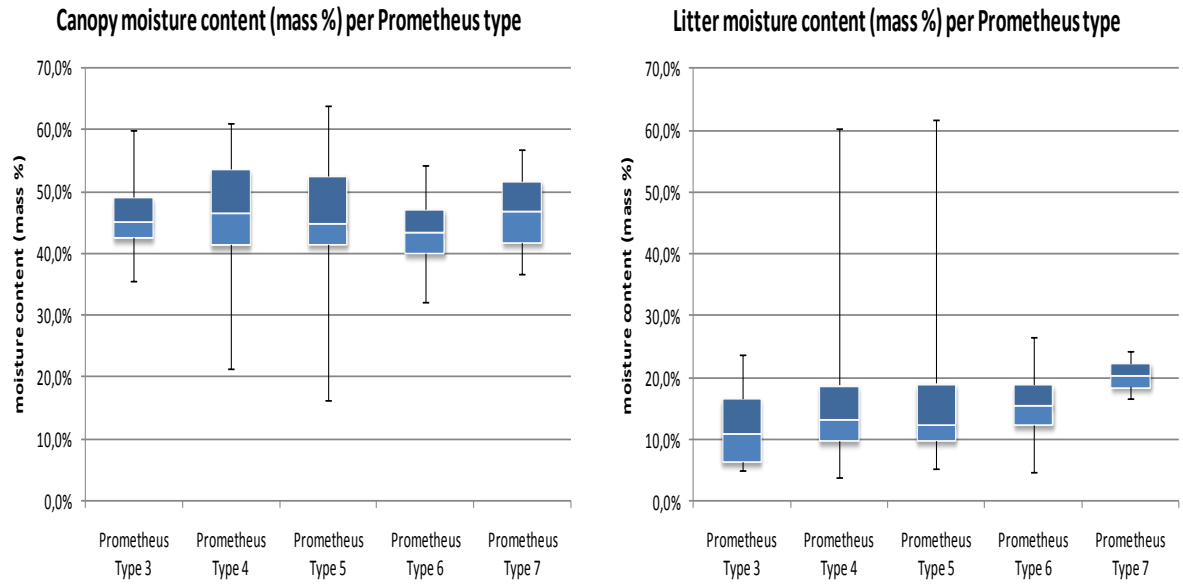

FIGURE 4.8 – BOX-WHISKER PLOT OF CANOPY (LEFT) & LITTER (RIGHT) MOISTURE CONTENT PER PROMETHEUS TYPE

Figure 4.9 shows the relation of moisture content with slope aspect (§1.1.3). Measured moisture content in the canopy samples was higher than in the litter samples. Across the entire aspect range, moisture levels did not produce an unambiguous relationship.

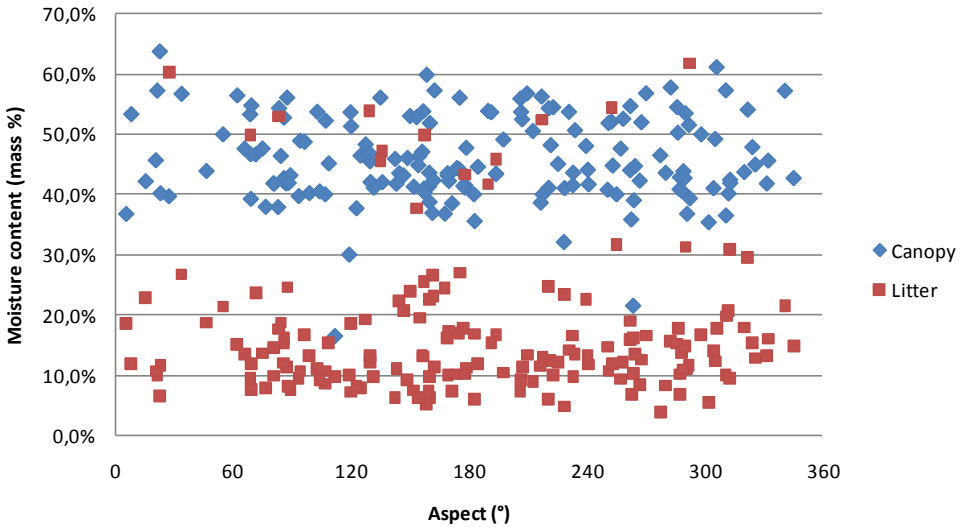

FIGURE 4.9 – SCATTERPLOT DEPICTING THE RELATION BETWEEN SLOPE ASPECT (X-AXIS) AND MEASURED MOISTURE CONTENT (Y-AXIS)

4.1.2 IMAGE CLASSIFICATION

As explained in §3.2.2, to be able to provide both the maximum likelihood and minimum distance to mean classifiers with equal inputs, the number of data bands needs to be 1 less than the number of observations of each Prometheus fuel type. Prometheus type 7 was only encountered two times; in order to include it in the analysis would require a reduction to only 1 data band. Although this one band would describe the largest amount of variance (as per Principal Component Analysis design), it was considered to be too much of a data loss and as a result, both occurrences of Prometheus type 7 were excluded from the dataset altogether. Prometheus type 6 was recorded 14 times, and as such the number of (PCA) databands used for both classification methods was 13.

Appendix H shows the result of the Maximum Likelihood classification, performed on the HyMap 2008 image. The maximum deviation allowed was set so that no pixels were left unclassified. The classification accuracies are given as a confusion (error) matrix in table 4.1. It was calculated by using the observed Prometheus types from all 164 plots (166 minus the two occurrences of Type 7) as validation data set on the classified HyMap image.

Nearly the entire study area is classified as either type 4 or type 5. Type 6 is present across the entire area, mostly as scattered pixels. Type 3 only takes the form of speckle, across the southeastern part of the study area. Areas with no vegetation are scarce, and mainly located in the parking areas surrounding the lower dam reservoir, and a few locations within the village of Vailhan. The extensive agricultural areas (vineyards) in the southeastern corner of the study area are not recognizable.

Overall accuracy = (126/164) 76.8 % Kappa coefficient = 0.63

	Ground Truth (pixels)					Producer	User
Class	PT 3	PT 4	PT 5	PT 6	**Total**	Accuracy	Accuracy
Unclassified	0	0	0	0	0		
PT 3	14	0	0	1	15	100.0 %	93.3 %
PT 4	0	23	5	1	29	54.8 %	79.3 %
PT 5	0	19	73	10	102	91.3 %	71.6 %
PT 6	0	0	2	16	18	57.1 %	88.9 %
Total	14	42	80	28	**164**		

TABLE 4.1 – CONFUSION MATRIX OF THE MAXIMUM LIKELIHOOD CLASSIFICATION

Appendix I shows the result of the Minimum Distance to Mean classification. Its confusion matrix is given in table 4.2, constructed in the same way as the previous one. As with the Maximum Likelihood classifier, the maximum distance allowed was set so that no pixels were left unclassified.

Compared with the result of the Maximum Likelihood classification, Type 4 and Type 5 are much more differentiated: the first is found mostly on the western side of the lake and river Peyne, while

the latter is found on the eastern side. The gullies leading to the lake, as well as large parts in the south of the study area, are classified as Type 4. As in the Maximum Likelihood classification, Type 6 occurs across the entire study area, but in larger congregations and always adjacent to Type 5 pixels. The No Vegetation/Agricultural class is much more abundant than in the Maximum Likelihood classification. The village of Vailhan, the small villages / farms in the northern part of the study area, and many of the agricultural fields in the southeast, clearly stand out.

Overall accuracy = (84/157) 53.5 % Kappa coefficient = 0.28

	Ground Truth (pixels)					Producer	User
Class	PT 3	PT 4	PT 5	PT 6	**Total**	Accuracy	Accuracy
Unclassified	0	0	0	0	0		
PT 3	5	4	1	0	10	45.5 %	50.0 %
PT 4	5	23	23	8	59	56.1 %	39.0 %
PT 5	0	11	51	13	75	64.6 %	68.0 %
PT 6	1	3	4	5	13	19.2 %	38.5 %
Total	11	41	79	26	**157**		

TABLE 4.2 – CONFUSION MATRIX OF THE MINIMUM DISTANCE TO MEAN CLASSIFICATION

Although the Maximum Likelihood classifier yielded an overall higher accuracy, the Minimum Distance to Mean classifier was still preferred in the end because its general appearance matched considerably better with the in-field experience with the study area. This was especially true for sections along the main roads and built-up areas. Also, the increased area of Prometheus type 4, mainly in the region west of the lake, was more in compliance with field observations.

4.1.3 VEGETATION RISK

The manual conversion of vegetation parameters into relative vegetation risk resulted in the assignment of risk classes to each of the four classified Prometheus types, as shown in Table 4.3. The risk value is the sum of all six percentages, multiplied by 2/3 to ensure a maximum value of 4. The resulting vegetation risk map is given in Appendix J.

average values	Primary Shrubs		Secondary Shrubs		Woody	Litter		
	cover	**alive**	**cover**	**alive**	**cover**	**cover**	**Risk value**	**Class**
P.Type 6	33.4%	78.9%	14.6%	84.7%	68.6%	76.8%	1.53	**3**
P.Type 5	10.1%	78.4%	1.4%	84.1%	63.4%	78.8%	1.27	**1**
P.Type 4	52.9%	77.0%	15.6%	76.7%	65.4%	71.8%	1.68	**4**
P.Type 3	64.6%	84.6%	26.7%	67.2%	43.2%	43.9%	1.51	**2**

TABLE 4.3 – CALCULATION OF RISK CLASSES FOR THE PROMETHEUS TYPES OF THE CLASSIFICATION

The highest risk class was assigned to Type 4, as it holds a high percentage of shrub coverage, combined with high volumes of ground fuel. Added to that is the fact that it comprises mainly shrubs

up to a height of 4 meters – there are very few mature trees present (<30 % canopy cover). The multitudes of small diameter stems are of much higher risk then would they be sizeable tree trunks. The lowest risk class was assigned to Type 5, as it holds by far the least amount of shrub coverage, basically resulting in only a significant risk concerning ground fires, which are much less severe then fire fronts of several meters in height associated with surface fires. Finally, type 6 received a higher risk class then type 3, as it contains much more (dead) ground material prone to ignition upon contact with either a glowing/sparking object, or lightning. Adjusting the influence of alive vegetation percentage only increased absolute differences in risk values: the relative order remained the same.

Since the vegetation risk values are directly coupled to the Prometheus types, the patterns in the vegetation risk map are equal to those in the Maximum Distance to Mean classification (appendix I). The highest risk class is found in south- and western parts of the study area. The eastern part has generally lower risk values.

4.2 HUMAN RISK MAP

Appendix K provides the human risk map. The edges of the roads surrounding the lake stand out clearly, as do the edges built up / agricultural areas north of the lake; indicating the ignition risk caused by machinery and burning or glowing material being thrown out of cars or by hikers (cigarettes). The picknick areas situated to the west and east of the lower dam basin, also pose a high risk in the bordering forest edges.

The multiple ‘dots’ visible in the northern half of the study area, are parts of the trails and footpaths situated throughout the forests. These tracks are narrow and often situated underneath the tree stands, hindering their visibility on imagery recorded from above. Because of pixel size (5x5 m) even parts of the main roads (which are ±5 m wide) are occluded from the classification due to their reflectance mixing with adjacent (or overhanging) vegetation.

The southern part is much more heterogeneous in nature: the dirt roads in the somewhat oval-shaped pine forest in the southeast are clearly distinguishable, but while most of the vineyards in the area correctly received their contour of increased risk, many individual spots remain unexplained.

4.3 TOPOGRAPHIC RISK MAP

Appendix L shows the result of the slope risk assessment. Due to the quadratic relationship of the slope factor, only a few steep (±40 %) slopes stand out from the abundant soft slopes (blue/green): a small area southeast of Pézenes-les-Mines and the three ‘hills’ to the west, southwest and southeast of Vailhan. Gullies directly to the north of Vailhan also contain relatively steep slopes. As for the rest

of the study area, the steepest slopes are found in the valley of the river Peyne and the various gullies leading towards the Peyne and Lac des Olivettes. Appendix M shows the result of the aspect risk assessment. South facing slopes received the highest risk class, north facing slopes the lowest risk class.

Combining the slope and aspect risk values resulted in the map shown Appendix N. As no clear relationship between aspect and moisture content were found (figure 4.9), no weight factors were included as the actual influence of aspect remained unclear. Nevertheless, because of the quadratic nature of the slope factor used to determine slope risk, emphasis in the combined risk would inherently be placed on slope steepness. The areas that stand out are the steep, south facing slopes.

4.4 COMBINED HAZARD MAP

The combination of the three risk factors (vegetation, human activity & topography), was performed with three different sets of weights:

	Vegetation	Human	Topography
Appendix O	1	1	1
Appendix P	1	$^{2}/_{3}$	$^{1}/_{3}$
Appendix Q	1	$^{3}/_{5}$	$^{1}/_{5}$

Choosing the weight factors was done by estimating the relative influence of the three factors. In the case of equal weights (appendix O), too much emphasis was being put on topography effects. As a result, differences in vegetation were suppressed. The clearest example of this is the pine forest in the southeastern part of the study area. With its high resin contents, and a thick layer of needle litter, it should pose one of the greatest hazards within the entire area. However, with equal weights, that severe hazard was strictly limited to the roads.

Appendices P and Q incorporate downscaled influences of both human and topographical risk. Vegetation remained the largest contributor to overall fire hazard, since the absence of fuel would simply remove the possibility of fire in its entirety. Human activity poses the largest risk of fire ignition. Hence its increased weight over topography. With the unclear relationship of aspect and fire risk, the influence of topography was reduced considerably, making it more if an indirect hazard: the potential severity *after* a fire is ignited is larger on steep slopes than on flat surfaces. The differences between thirds (appendix P) and fifths (appendix Q) as weights is small. The added influence of topography in the first merely tones down the influence of vegetation on the overall hazard image.

The most severe hazards are found in the pine forest in the southeastern part of the study area, and to the west and south of the lake, where the vegetation mainly consists of Prometheus type 4 (high

amount of shrubs and woody fuel / litter). Buildings, parking lots and agricultural areas stand out as dark green, low risk spots. Their edges pose a strong increase in fire hazard, consistent with for instance the picknick areas near the lower dam basin: low risk on the asphalt/gravel itself, and a high risk in the surrounding vegetation, where glowing embers or coals would most likely be dumped. Although intermittently appearing on the map, due to overhanging vegetation, the main roads and hiking / hunting tracks are also visible as red lines throughout the area. In the north and northwestern parts of the study area, the lower risks associated with Prometheus types 5 and 6 vegetation (lower amounts of shrubs, mainly trees with sizeable trunks), result in a light shade of green.

5 DISCUSSION

During the fieldwork, Prometheus types 3, 4, 5, 6 and 7 were encountered. During the creation of the vegetation risk map, the two occurrences of type 7 were omitted, to allow the classification methods to be used on more than 1 data band. The final vegetation risk was not computed by means of the FCCS, but by manually assigned risk values (classes) based on shrub, woody fuels and litter cover. No clear pattern emerged from the measured moisture content of canopy and litter samples. To create the final maps, the three risk factors (vegetation, human activity and topography) were weighed according to their influence on the overall fire hazard.

5.1 VEGETATION RISK

Reviewing the methods contained within the FCCS's (§3.1.2), a conceptual risk factor was constructed, based on the six measured variables mentioned in §3.2.3. As the vast majority of the plots with canopy data consisted of multiple mature trees of which the trunks are too thick to be prone to either direct ignition or even small to medium existing fires, the canopy (cover-) data was left out of the risk value calculations. Furthermore, with human activity being by far the most common source of ignition, especially along roadsides, ignition of the (moist) canopy was considered highly unlikely. Instead, the risk in strata lower to the ground (shrub level) was favored.

Cover was assumed to be more directly related to fire hazard than biomass. While biomass would eventually cause a fire to burn longer and more severe, its relationship towards fire *ignition* is not clearly distinguishable (or described in literature). In the FCCS, biomass is included in the calculations, and for instance used to determine the flamelengths and CO_2 production of the fueltype under consideration. Furthermore, cover is much more indicative of the 'connectivity' of the vegetation: a single tree can still provide a lot of biomass to burn, but if there is no additional vegetation nearby, it would simply burn out and the fire would not spread. Again, if that same amount of biomass would be divided over a stand of vegetation with interlocking canopies/branches (such as the post-logging, regenerated forest patches encountered in the study area), the risk of the fire rapidly spreading after ignition is far greater. This would then be indicated by a (much) higher cover fraction.

The approach taken in order to create the vegetation risk map, by computing average risk values per Prometheus type, results in a certain amount of generalization. By then classifying these average values in the 5 fixed classes, false relative differences were created between the classes. While this does result in a more contrast-rich overall hazard map, it would have been more appropriate to use the values of the six used parameters *directly* for the classification of the entire area. That way, a map of vegetation risk values can be produced, that is truly comparable with the other risk maps.

However, the exclusion of the canopy data from the calculations did more or less prohibit the use of remotely sensed images to directly map the six parameter's values: these strata lie mostly obscured from view, underneath the canopy layers. Hence the indirect approach of parameterizing the individual Prometheus types, after their classification. Arroyo *et al.* (2006) used object-oriented classification, instead of the pixel orientated method used in this research, to classify the Prometheus types. The accuracy of the resulting map was assessed to be above 80% when compared with field observations. While other classification techniques may thus improve the classification process of the Prometheus types, that does not readily provide a quantification of the risk posed by the assigned fuel type, as *is* included in the FCCS (e.g. Ottmar *et al.,* 2007).

5.2 HUMAN RISK

As for the human risk assessment, the challenge was to 'distill' the manmade structures from the available imagery. To this end, the choice was between the use of satellite imagery and topographic maps of the area. The main advantage of the satellite images is that they can be more easily updated if needed, and will thus provide a more up to date status of an area in terms of land use. The major shortcoming of satellite images is the inability to "see" roads, buildings or footpaths underneath vegetation (or under anything else for that matter). For example, electricity facilities are often small and tucked away near edges of villages. While they pose a great risk of ignition when in the close vicinity of vegetation, they are mostly invisible on satellite images and as such will not be incorporated into the risk assessment.

Satellite imagery was chosen as the source of classification, but this inevitably lead to inconsistencies. River beds marked as roads or buildings, actual roads marked only intermittently – even the major ones - presumably caused by either grid cell size (5m) and/or or overgrowth, and large stretched of land marked as agricultural in the southern parts of the area. Although practically undocumented in existing literature, (thematic) topographic maps could maybe be used as an alternative source. Either in digital form, for direct classification, or by manually digitalizing the needed features from a hardcopy version. Its success would depend on the quality and contents of the maps available.

While agricultural lands pose no real vegetation risk, they bring about a lot of other activity, such as machinery, workmen, and the occasional burning down of crops to clear the land. Hence they are rightfully shown on the human risk map. While the human risk map classified the roads and tracks – where visible from above – fairly well, what is not incorporated was the intensity with which each road is used. It stands to reason that the main roads, frequently used by local inhabitants, would be

associated with a greater risk of ignition than a rarely used footpath up in the hills. On the other hand, these small trail would be frequently used by hunters. All in all, the exact differences in human risk for different classes of roads and tracks would be difficult to map. Again, classification by means of topographical maps could provide an already made subdivision into road (use) classes.

5.3 TOPOGRAPHICAL RISK

No clear relation was discovered out of the canopy and litter moisture content and slope aspect (figure 4.9). This would then lead to believe there is no real influence of aspect on fuel moisture content. As for litter moisture, this may be due to the fact that the undergrowth is shielded from direct sunlight by the canopy, on both northern and southern slopes alike. Similarly, the absence of a relationship in canopy moisture could be explained by the samples being taken from the base of the canopy, rather than the top of the canopy. However, during the fieldwork, attention was paid to this effect, and all samples were consistently taken from branches with direct exposure to the sun.

Despite all reservations regarding aspect, some level of effect is still to be expected on ignition risk. Especially in an area full of relief such as the study area, twilight periods are relatively short, resulting in a difference between the southern and northern exposed slopes in terms of drying up after a rain event for example. Evidently, this might then only affect crown ignition risk, but to make the topographical risk that bit more dynamic, aspect was incorporated nevertheless – albeit with a reduced influence.

5.4 WEATHER

The fourth component, that was to be originally included in the combined hazard map, was short-term meteorological data. Temperature, humidity and precipitation form the most dynamic, perhaps most important, data source for a complete assessment of fire hazard. However, on the relatively small scale of the study area under consideration, spatial variations in temperature and humidity will most likely be rare.

Depending on the extent of precipitation, i.e. where the borderline between dry and wet is located, great local differences can occur in the amount of precipitation within the relatively small study area. In an overall dry summer period, all types of areas will be at a higher risk, as all available fuel will be drier. An ignition source (e.g. a cigarette or barbecue coals) will then have a greater chance of starting a fire. Under low humidity conditions, both ignition and propagation of a fire will be sped up across all types.

Maybe in future, a direct feed from meteorological systems can be used as an overlay on top of the pre-existing, static, differences in fire hazard (the combined hazard map). In doing so, areas that reach a certain threshold can be identified quicker and more accurately then when only a general indication for the entire area is provided.

5.5 COMBINED FIRE HAZARD

Caution is needed in judging the combined hazard maps: They do *not* imply that areas assigned a low risk value have no fire hazard; the risk values shown on these maps provide an indication of the risk relative to other areas *within* the study area. The numerical representation may be misleading in this respect, but such is the result of using a mathematical approach based on methods of the FCCS. Should the FCCS be further updated or adapted in the future, it could be possible to change the vegetation specific properties to match those of the European Mediterranean region, and to use the full extent of paramaters contained within it to calculate comparable, absolute differences in hazard.

Nonetheless, the FCCS is the only method found in literature that quantifies certain potentials of a forest fire (Ottmar *et al.*, 2007; Riccardi *et al.*, 2007b). For instance, Martinez *et al.* (2009) provide information on human risks, but only do so by assigning either *high* or *low* categories. The FCCS, however, focuses on vegetation risk, and does not provide any information on how to combine separate values for vegetation risk, human risk and / or topographic risk. In this respect, no reference material was available at the time of this writing.

Overall fire hazard is the sum of all individual components. Varying the weights of each of the three components, in order of expected influence (§3.5), instead of them all having equal influence, results in a map that is more representative of the conditions in the study area (§4.4). As roads, villages and other manmade structures, in a relief-rich area like this, are usually cut out from hill slopes, human risk and topographical risk will reinforce each other, justifying the stronger influence given to the vegetation risk value.

While high risk areas caused by human activity have an obvious need for attention (and prevention), high risk by means of natural causes can be manipulated by methods also incorporated in the FCCS (Ottmar *et al.*, 2007). Whereas it would be difficult to change slope or aspect of a location, vegetation type can indeed be influenced. Ground fuels can be cleared, or even burnt down in a controlled manner as to remove fuels from the system. Also, as thicker, more solitary trees provide less fire hazard than tightly packed shrubs, thinning out a currently high risk area by removing (undergrowth) vegetation and/or logging debris might very well be an effective way of reducing fire hazard (Keane *et al.*, 2000; Martinez *et al.*, 2009).

6 CONCLUSIONS

By combining literature, fieldwork, remotely sensed imagery and GIS software, it is possible to create a reliable fire hazard map of the Peyne area. In accordance with expectations, it shows the highest risk areas to coincide with the most prone vegetation types, and human activities encountered in the area.

Vegetation risk could be mapped by means of remote sensing, by classifying the encountered Prometheus types. Omitting the assigned categories (between 0 and 4), and instead using the calculated values directly for classification may improve the overall representation of vegetation risk. While the minimum distance to mean classifier resulted in an overall less accurate classification, the resulting map was more in accordance with field experience than that resulting from the maximum likelihood classification. Object orientated classification methods may also provide better results.

Human risk was successfully mapped from topographic maps of the area and an NDVI image (used mainly to select unvegetated areas). Parts of the roads, especially footpaths in the forests, lie underneath the forest canopy and are thus invisible from above. Where visible on the satellite imagery, most of the features associated with human activity were successfully classified. The use of existing topographical maps in classifying human activity types would not only help in mapping the intermittently visible roads and tracks, and completely invisible (due to their size) electrical structures, but also be an improvement over the generalization that was now present within this map (e.g. no difference in road use intensities). Again, object orientated classification methods could also provide useful in this respect.

Risk caused by terrain was determined by both slope and aspect; two parameters that were easily extracted from the existing digital elevation model. Converting slope steepness into an increase of fire hazard (spread rate) could be done directly by using a formula from the FCCS. Due to its unclear relationship with fuel moisture level, the final influence of aspect was reduced considerably.

The final, overall hazard map was created by combining the vegetation, human, and topographical risk maps into one, each with its own weight factor. Weight factors of $^{3}/_{5}$ and $^{1}/_{5}$ for the human and topographical risk respectively, were preferred over weight factors of $^{2}/_{3}$ and $^{1}/_{3}$, due to the increased emphasis on vegetation provided by the first combination. Equal weights for all three factors resulted in a map where high risk areas would not necessarily have any fuel available.

Reviewing the existing literature, the assessment of forest fire hazard by means of quantifiable parameters such as present within the Fuel Characteristic Classification System, has never been applied to the creation of actual maps. The calculated potentials have been used as separate

outcomes, for instance to create fuel maps or hazardous locations based on human activity, but not as a combined property. The combinations of several individual influences on fire hazard, into a single map, can provide insights into relationships between the factors themselves, and how they reinforce or perhaps weaken each other. Since overall fire hazard is ultimately determined by multiple factors, changing one of them could very well lead to the desired reduction of wildfires.

Maybe in future, a direct feed from meteorological systems (precipitation, temperature, humidity, wind speed and direction) can be used as an overlay on top of the pre-existing, static, differences in fire hazard (the combined hazard map). In doing so, areas that reach a certain hazard threshold can be identified quicker and more accurately then when only a general indication for the entire area is provided.

7 REFERENCES

ALBINI, F.A. (1976). Estimating wildfire behavior and effects, - *Gen.Tech. Rep. INT-30.* Ogden, UT: U.S. Derpartment of Agriculture, Forest Service, Intermountain Forest and Range Experiment Station, pp. 92.

ANDERSON, H.E. (1982). Aids to Determining Fuel Models For Estimating Fire Behavior, - *Gen.Tech. Rep. INT-122.* Ogden, UT: U.S. Derpartment of Agriculture, Forest Service, Intermountain Forest and Range Experiment Station, pp 22.

ARROYO, L.A., HEALEY, S.P., COHEN, W.B., COCERO, D., MANZANERA, J.A. (2006). Using object-orientated classification and high-resolution imagery to map fuel types in a Mediterranean region, - *Journal of Geophysical Research,* ***111,*** G04S04.

BARRETT, T.M, ZUURING, H.R., CHRISTOPHER, T. (2007). Interpretation of forest characteristics from computer-generated images, - *Landscape and Urban Planning,* ***80,*** 396-403.

BROWN, J.K. (1971). A planar intersect method for sampling fuel volume and surface area, - *Forest Science,* ***17 (1),*** 96-102.

BROWN, J.K. (1974). Handbook for inventorying downed woody material, - *Gen.Tech. Rep. INT-16.* U.S. Department of Agriculture, Forest Service, pp 24.

CARNIA, A., SAN-MIGUEL-AYANZ, J., KUCERA, J., AMATULLI, G., BOCA, R., LIBERTÀ, G., DURRANT, T., SCHMUCK, G., SCHULTE, E., BUCKI, M. (2008). Forest fires in Europe - 2007, - European Commission, Joint Research Centre, Institute for Environment and Sustainability. *Luxembourg: Office for Official Publications of the European Communities****, EUR 23492 EN****,* pp. 77.

CHUVIECO, E. & CONGALTON, R.G. (1988). Mapping and Inventory of Forest Fire from Digital Processing of TM Data, - *Geocarto International,* ***4,*** 41-53.

DARMAWAN, M., ANIYA, M., TSUYUKI, S. (2001). Forest Fire Hazard Model Using Remote Sensing and Geographic Information Systems: Toward understanding of Land and Forest Degradation in Lowland areas of East Kalimantan, Indonesia, - *22nd Asian Conference on Remote Sensing, 5-9 November 2001, Singapore,* Topic B4.

DE ALBUQUERQUE, L.M.M., PARANHOS FILHO, A.C., TORRES, T.G., KASSAR, E., DE MATOS FILHO, H.J.S., CARRIJO, M.G.G., PAVÃO, H.G., DE SOUZA, A. (2007). Subsides to the creation of a regional model of forest fire hazard: Taquari River Springs Park, MS – A case study, - *Atmospheric Environment,* ***41,*** 3494-3501.

DENNISON, P.E., ROBERTS, D.A., THORGUSEN, S.R., REGELBRUGGE, J.C., WEISE, D., LEE, C. (2003). Modeling seasonal changes in live fuel moisture and equivalent water thickness using a cumulative water balance index, - *Remote Sens. of Environment,* ***88,*** 442-452.

GAO, B.C. (1996). NDWI – A normalized difference water index for remote sensing of vegetation liquid water from space, - *Remote Sensing of Environment,* ***58,*** 257-266.

GEZE, B., (1979). Languedoc : Mediterraneen, Montagne Noire. Paris : Masson, pp 191.

GRISHIN, A.M. & SHIPULINA, O.V. (2002). Mathematical Model for Spread of Crown Fires in Homogeneous Forests and along Openings, - *Combustion, Explosion, and Shock Waves,* ***Vol. 38, No. 6,*** 622-632.

ISABELLA BOVOLO, C., ABELE, S.J., BATHURST, J.C., CABALLERO, D., CIGLAN, M., EFTICHIDIS, G., SIMO, B. (2009). A distributed framework for multi-risk assessment of natural hazards used to model the effects of forest fire on hydrology and sediment yield, - *Computers & Geosciences,* ***35,*** 924-945.

KEANE, R.E., MINCEMOYER, S.A., SCHMIDT, K.M., LONG, D.G., GARNER, J.L. (2000). Mapping vegetation and fuels for fire management on the Gila National Forest Complex, New Mexico, [CD-ROM]- *Gen. Tech. Rep. RMRS-GTR-46-CD.* Ogden, UT: U.S. Department of Agriculture, Forest Service, Rocky Mountain Research Station, pp 126.

KESSELL, S.R., POTTER, M.W., BEVINS, C.D., BRADSHAW, L., JESKE, B.W. (1978). Analysis and Application of Forest Fuels Data, - *Environmental Management, **Vol.2, No. 4**,* 347-363.

KRASNOW, K., SCHOENNAGEL, T., VEBLEN, T.T. (2009). Forest fuel mapping and evaluation of LANDFIRE fuel maps in Boulder County, Colorado, USA, - *Forest Ecology and Management, **257**,* 1603-1612.

LAMPIN-MAILLET, C., JAPPIOT, M., LONG, M., MORGE, D., FERRIER, J.-P. (2009). Characterization and mapping of dwelling types for forest fire prevention, - *Computers, Environment and Urban Systems, **33**,* 224-232.

LANORTE, A. & LASAPONARA, R. (2007). Fuel type characterization based on coarse resolution MODIS satellite data, - *Forest@, **4 (2)**,* 235-243.

LASAPONARA, R. & LANORTE, A. (2007). Remotely sensed characterization of forest fuel types by using satellite ASTER data, - *International Journal of Applied Earth Observation and Geoinformation, **9**,* 225-234.

LILLESAND, T.M., KIEFER, R.W., CHIPMAN, J.W. (2004). Remote Sensing and Image Interpretation, - *5th Edition.* Hoboken, NJ: John Wiley & Sons Inc., pp 763.

MARTINEZ, J., VEGA-GARCIA, C., CHUVIECO, E. (2009). Human-caused wildfire risk rating for prevention planning in Spain, - *Journal of Environmental Management, **90**,* 1241-1252.

MCKENZIE, D., RAYMOND, C.L., KELLOGG, L.-K.B., NORHEIM, R.A., ANDREU, A.G., BAYARD, A.C., KOPPER, K.E., ELMAN, E. (2007). Mapping fuels at multiple scales: landscape application of the Fuel Characteristic Classification System, - *Canadian Journal of Forest Research, **37**,* 2421-2437.

MERRILL, D.F. & ALEXANDER, M.E. (1987). Glossary of forest fire management terms, - *National Research Council of Canada, Committee for Forest Fire Management, Ottawa.*

OTTMAR, R.D., SANDBERG, D.V., RICCARDI, C.L., PRICHARD, S.J. (2007). An overview of the Fuel Characteristic Classification System – Quantifying, classifying, and creating fuelbeds for resource planning, - *Canadian Journal of Forest Research, **37**,* 2383-2393.

RADLOFF, D.L., SCHOPFER, W.C., YANCIK, R.F. (1982). Slash Fire Hazard Analysis on the Siskiyou National Forest, - *Environmental Management, **Vol. 6, No.6**,* 517-526.

RIAÑO, D., CHUVIECO, E., SALAS, J., PALACIOS-ORUETA, A., BASTARRIKA, A. (2002). Generation of fuel type maps from Landsat TM images and ancillary data in Mediterranean ecosystems, - *Canadian Journal of Forest Research, **32**,* 1301-1315.

RICCARDI, C.L., OTTMAR, R.D., SANDBERG, D.V., ANDREU, A., ELMAN, E., KOPPER, K., LONG, J. (2007A). The fuelbed: a key element of the Fuel Characteristic Classification System, - *Canadian Journal of Forest Research, **37**,* 2394-2412.

RICCARDI, C.L., PRICHARD, S.J., SANDBERG, D.V., OTTMAR, R.D. (2007B). Quantifying physical characteristics of wildland fuels using the Fuel Characteristic Classification System, - *Canadian Journal of Forest Research, **37**,* 2413-2420.

ROBERTS, D.A., GREEN, R.O., ADAMS, J.B. (1997). Temporal and spatial patterns in vegetation and atmospheric properties from AVIRIS, - *Remote Sensing of Environment, **62**,* 223-240.

ROBERTS, D.A., DENNISON, P.E., PETERSON, S., SWEENEY, S., RECHEL, J. (2006). Evaluation of Airborne Visible/Infrared Imaging Spectrometer (AVIRIS) and Moderate Resolution Imaging Spectrometer (MODIS) measures of live fuel moisture and fuel condition in a shrubland ecosystem in southern California, - *Journal of Geophysical Research,* ***111,*** G04S02.

ROTHERMEL, R.C. (1972). A mathematical model for fire spread predictions in wildland fuels. - *Research Paper INT-115.* Ogden, UT: U.S. Department of Agriculture, Forest Service, Intermountain Forest and Range Experiment Station. pp 40.

SANDBERG, D.V., RICCARDI, C.L., SCHAAF, M.D. (2007A). Reformulation of Rothermel's wildland fire behaviour model for heterogeneous fuelbeds, - *Canadian Journal of Forest Research,* ***37,*** 2438-2455.

SANDBERG, D.V., RICCARDI, C.L., SCHAAF, M.D. (2007B). Fire potential rating for wildland fuelbeds using the Fuel Characteristic Classification System, - *Canadian Journal of Forest Research,* ***37,*** 2456-2463.

SCHAAF, M.D., SANDBERG, D.V., SCHREUDER, M.D., RICCARDI, C.L. (2007). A conceptual framework for ranking crown fire potential in wildland fuelbeds, - *Canadian Journal of Forest Research,* ***37,*** 2464-2478.

SCOTT, J.H. & BURGAN, R.E. (2005). Standard Fire Behavior Fuel Models: A Comprehensive Set for Use with Rothermel's Surface Fire Spread Model, - *Gen. Tech. Rep. RMRS-GTR-153.* Fort Collins, CO: U.S. Department of Agriculture, Forest Service, Rocky Mountain Research Station. pp 72.

SCOTT, J.H. & REINHARDT, E.D. (2001). Assessing crown fire potential by linking models of surface and crown fire behavior, - *Research Paper RMRS-RP-29.* Fort Collins, CO: U.S. Department of Agriculture, Forest Service, Rocky Mountain Research Station. pp 59.

SLUITER, R. (2005). Mediterranean land cover change: modelling and monitoring natural vegetation using GIS and remote sensing. *Netherlands Geographical Studies 33,3 Utrecht*. pp 145.

SYPHARD, C., RADELOFF, V.C., KEELEY, J.E., HAWBAKER, T.J., CLAYTON, M.K., STEWART, S.I., HAMMER, R.B. (2007). Human influence on California fire regimes, - *Ecological Applications,* ***17 (5),*** 1388-1402.

VAN WAGNER, C.E. (1977). Conditions for the start and spread of crown fire, - *Canadian Journal of Forest Research,* ***7,*** 23-34.

TÜRKER, M.F. (2005). A critical approach to the calculation method of economic value of forest fire damages in Turkish forestry: A case of forest enterprise from the Mediterranean region, - *International Forest Fire News,* ***33,*** *july - december,* 82-87.

VAN WAGNER, C.E. (1993). Prediction of crown fire behavior in two stands of jack pine, - *Canadian Journal of Forest Research,* ***23,*** 442-449.

VIDAL, A. & DEVAUX-ROS, C. (1995). Evaluating forest fire hazard with a Landsat TM derived water stress index, - *Agricultural and Forest Meteorology,* ***77,*** 207-224.

WESTFALL, J.A. & WOODALL, C.W. (2007). Measurement repeatability of a large-scale inventory of forest fuels, - *Forest Ecology and Management,* ***253,*** 171-176.

Lac des Olivettes and surroundings

La Peyne catchment, Southern France

Topographic map 1:25.000

Grid: UTM (WGS-1984 31T)

Sources:
Top - Michelin Top 25 - 2643 OT (2001)
Bottom - Michelin Série Bleu - 2644 O (1990)

K.A. Gortmaker
R.R.R. Oerlemans
R.P. Vink

June 25th, 2009

N

0 250 500 1,000 Meters

520000 521000 522000 523000 524000 525000 526000 527000 528000 529000

4827000 4826000 4825000 4824000 4823000 4822000 4821000

Utrecht University
Faculty of Geosciences
Department of Physical Geography

Lac des Olivettes and surroundings

La Peyne catchment, Southern France

Digital Elevation Model 1:25.000

Grid: UTM (WGS-1984 31T)

Sources:
BD Topo MNT. IGN PARIS - La Peyne (2001)
Top - Michelin Top 25 - 2643 OT (2001)
Bottom - Michelin Série Bleu - 2644 O (1990)

K.A. Gortmaker
R.R.R. Oerlemans
R.P. Vink

June 25th, 2009

N

0 250 500 1,000 Meters

StudyArea

+m MSL

478

99

Utrecht University
Faculty of Geosciences
Department of Physical Geography

520000 521000 522000 523000 524000 525000 526000 527000 528000 529000

4827000 4826000 4825000 4824000 4823000 4822000 4821000

Lac des Olivettes and surroundings

La Peyne catchment, Southern France

NDVI map 1:25.000

Grid: UTM (WGS-1984 31T)

Sources:
HyMap 2008 Caux - D908 (Carlencas)
Top - Michelin Top 25 - 2643 OT (2001)
Bottom - Michelin Série Bleu - 2644 O (1990)

K.A. Gortmaker
R.R.R. Oerlemans
R.P. Vink

June 25th, 2009

N

0 250 500 1,000 Meters

NDVI

0.94

0.67

Utrecht University
Faculty of Geosciences
Department of Physical Geography

520000 521000 522000 523000 524000 525000 526000 527000 528000 529000

4827000 4826000 4825000 4824000 4823000 4822000 4821000

Lac des Olivettes and surroundings

La Peyne catchment, Southern France

Planned plot locations 1:25.000

Grid: UTM (WGS-1984 31T)

Sources:
Top - Michelin Top 25 - 2643 OT (2001)
Bottom - Michelin Série Bleu - 2644 O (1990)

K.A. Gortmaker
R.R.R. Oerlemans
R.P. Vink

July 8th, 2009

N

0 250 500 1,000 Meters

Utrecht University
Faculty of Geosciences
Department of Physical Geography

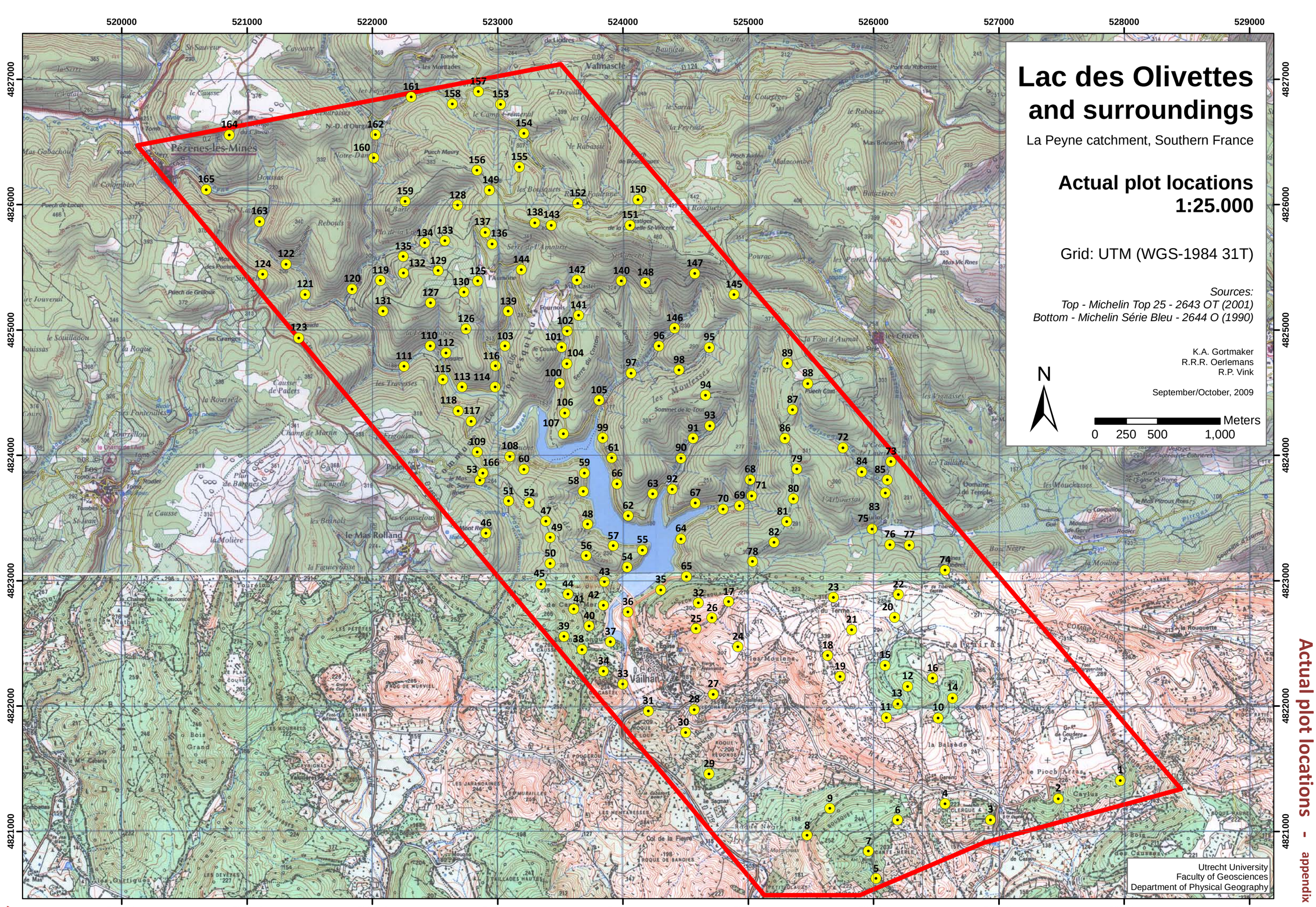
Lac des Olivettes
and surroundings
La Peyne catchment, Southern France
Actual plot locations
1:25.000
Grid: UTM (WGS-1984 31T)
Sources:
Top - Michelin Top 25 - 2643 OT (2001)
Bottom - Michelin Série Bleu - 2644 O (1990)
K.A. Gortmaker
R.R.R. Oerlemans
R.P. Vink
September/October, 2009
N
0 250 500 1,000 Meters
Utrecht University
Faculty of Geosciences
Department of Physical Geography
520000
521000
522000
523000
524000
525000
526000
527000
528000
529000
4827000
4826000
4825000
4824000
4823000
4822000
4821000

Date	- -	X (UTM)		Slope	°	Plot size	Plot nr.
Time	:	Y (UTM)		Aspect	°		
Weather		Z (m)		Prometheus Type			

Samples	Total (g)	Dried (g)	Moisture
Canopy / Shrub			%
Litter (ft^2)			%

Photo #		
Hemi #		

Canopy

Total cover	% (observed)
	% (Hemisph.)

	Cover (%)	# / plot
Overstory		
Midstory		
Understory		

Remarks (e.g. ladder fuels):

#	Over/Mid Understory	Height (m)	Height live crown (m)	CBH (cm)	Species	Basal accumulation		
						depth	radius	type
1								
2								
3								
4								
5								
6								
7								
8								
9								
10								
11								
12								
13								
14								
15								
16								
17								
18								
19								
20								
21								
22								
23								
24								
25								

#	Snags / Stumps	Height (m)	# / plot	CBH (cm)	Species
1					
2					
3					
4					
5					
6					

Snags
class 1 - foliage present
class 1 - foliage absent
class 2 - branches & bark
class 3 - rotten, no branches & bark
Stumps
Sound / Rotten

Ladder fuels	*min height (m) | max height (m) | type (lichens/moss ; climbing plants ; dead branches ; leaning snags ; stringy/fuzzy bark ; tree regeneration ; vines/liana)*
Basal acc.	*bark | branches | broadleaf deciduous | broadleaf evergreen | grass | needles | palm fronds*

Shrubs

	cover (%)	height (m)	amount live	Species
primary			%	
secondary			%	

Remarks:

Non Woody

	cover (%)	height (m)	amount live	Loading kg / ft^2	Species
primary			%		
secondary			%		

Remarks:

Woody

cover (%)	depth (cm)

Sample	Class most abundant	Total (g)	Dried (g)	Avg. Weight /element (g)
	-			
	3 elements: nearest to origin & transect ends			

Sound (cm)	# / upslope transect	# / crossslope transect	Species
0 - 0.64			
0.64 - 2.54			
2.54 - 7.62			
7.62 - 22.86			
22.86 - 50.8			
> 50.8			
Rotten (cm)	# / upslope transect	# / crossslope transect	Species
7.62 - 22.86			
22.86 - 50.8			
> 50.8			

Remarks:

Ground Lichen

cover (%)	depth (cm)

Moss

cover (%)	depth (cm)

Type: sphagnum other

Litter

cover (%)	depth (cm)

Arrangement: fluffy normal perched

Type	%	Type	%
Short needle		Deciduous	
Long needle		Evergreen	
Conifer		Grass	
Palm frond			

Remarks:

Ground

	rotten wood (%)	
	cover (%)	depth (cm)
Upper		
Lower		

Type: moss/litter sphagnum (Partially decomposed)

Type: moss/litter sphagnum (Fully decomposed)

Remarks:

Lac des Olivettes and surroundings

La Peyne catchment, Southern France

Observed Prometheus Types 1:25.000

Grid: UTM (WGS-1984 31T)

Sources:
Top - Michelin Top 25 - 2643 OT (2001)
Bottom - Michelin Série Bleu - 2644 O (1990)

N

K.A. Gortmaker

September/October, 2009

0 250 500 1,000 Meters

StudyArea

Observed Prometheus Type

- Type 3 (>60% shrubs 0.6-2.0 m; <50% trees)
- Type 4 (>60% shrubs 2.0-4.0 m; <50% trees)
- Type 5 (<30% shrubs; >50% trees >4 m)
- Type 6 (>30% shrubs; >50% trees >4 m; medium understory)
- Type 7 (>30% shrubs; >50% trees >4 m; heavy understory)

Utrecht University
Faculty of Geosciences
Department of Physical Geography

520000 521000 522000 523000 524000 525000 526000 527000 528000 529000

4827000 4826000 4825000 4824000 4823000 4822000 4821000

Lac des Olivettes and surroundings

La Peyne catchment, Southern France

Prometheus Types

Maximum Likelihood Classification

1:25.000

Grid: UTM (WGS-1984 31T)

Sources:
BD Topo MNT. IGN PARIS - La Peyne (2001)
Top - Michelin Top 25 - 2643 OT (2001)
Bottom - Michelin Série Bleu - 2644 O (1990)

N

K.A. Gortmaker

April, 2010

Meters
0 250 500 1,000

Maximum Likelihood Classification

- StudyArea
- Prometheus Type 3
- Prometheus Type 4
- Prometheus Type 5
- Prometheus Type 6
- Water
- No Vegetation/Agricultural

Utrecht University
Faculty of Geosciences
Department of Physical Geography

520000 521000 522000 523000 524000 525000 526000 527000 528000 529000

4827000 4826000 4825000 4824000 4823000 4822000 4821000

Lac des Olivettes and surroundings

La Peyne catchment, Southern France

Prometheus Types

Minimum Distance to Mean Classification

1:25.000

Grid: UTM (WGS-1984 31T)

Sources:
BD Topo MNT. IGN PARIS - La Peyne (2001)
Top - Michelin Top 25 - 2643 OT (2001)
Bottom - Michelin Série Bleu - 2644 O (1990)

N

K.A. Gortmaker

April, 2010

Meters
0 250 500 1,000

Minimum Distance to Mean Classification

- StudyArea
- Prometheus Type 3
- Prometheus Type 4
- Prometheus Type 5
- Prometheus Type 6
- Water
- No Vegetation/Agricultural

Utrecht University
Faculty of Geosciences
Department of Physical Geography

520000 521000 522000 523000 524000 525000 526000 527000 528000 529000

4827000 4826000 4825000 4824000 4823000 4822000 4821000

Lac des Olivettes and surroundings

La Peyne catchment, Southern France

Vegetation Risk 1:25.000

Grid: UTM (WGS-1984 31T)

Sources:
BD Topo MNT. IGN PARIS - La Peyne (2001)
Top - Michelin Top 25 - 2643 OT (2001)
Bottom - Michelin Série Bleu - 2644 O (1990)

K.A. Gortmaker

April, 2010

N

0 250 500 1,000 Meters

StudyArea

Risk class

- 0 (No Vegetation / Agricultural) - None
- 1 - Low
- 2
- 3
- 4 - High

Utrecht University
Faculty of Geosciences
Department of Physical Geography

Vegetation risk map - appendix J

Lac des Olivettes and surroundings

La Peyne catchment, Southern France

Human Risk 1:25.000

Grid: UTM (WGS-1984 31T)

Sources:
BD Topo MNT. IGN PARIS - La Peyne (2001)
Top - Michelin Top 25 - 2643 OT (2001)
Bottom - Michelin Série Bleu - 2644 O (1990)

N

K.A. Gortmaker

March, 2010

0 250 500 1,000 Meters

520000 521000 522000 523000 524000 525000 526000 527000 528000 529000

4827000 4826000 4825000 4824000 4823000 4822000 4821000

StudyArea

Risk class

High : 4.0

Low : 0.1

0 - No risk

Utrecht University
Faculty of Geosciences
Department of Physical Geography

Lac des Olivettes and surroundings

La Peyne catchment, Southern France

Slope Risk 1:25.000

Grid: UTM (WGS-1984 31T)

Sources:
BD Topo MNT. IGN PARIS - La Peyne (2001)
Top - Michelin Top 25 - 2643 OT (2001)
Bottom - Michelin Série Bleu - 2644 O (1990)

N

K.A. Gortmaker

January 5th, 2010

0 250 500 1,000 Meters

520000 521000 522000 523000 524000 525000 526000 527000 528000 529000

4827000 4826000 4825000 4824000 4823000 4822000 4821000

StudyArea

Slope Risk

High : 4

Low : 0

Utrecht University
Faculty of Geosciences
Department of Physical Geography

Lac des Olivettes and surroundings

La Peyne catchment, Southern France

Aspect Risk
1:25.000

Grid: UTM (WGS-1984 31T)

Sources:
BD Topo MNT. IGN PARIS - La Peyne (2001)
Top - Michelin Top 25 - 2643 OT (2001)
Bottom - Michelin Série Bleu - 2644 O (1990)

N

K.A. Gortmaker

January 5th, 2010

0 250 500 1,000 Meters

520000 521000 522000 523000 524000 525000 526000 527000 528000 529000

4827000 4826000 4825000 4824000 4823000 4822000 4821000

StudyArea

Aspect Risk

High (S): 4

Medium (E/W): 2

Low (N): 0

Utrecht University
Faculty of Geosciences
Department of Physical Geography

Lac des Olivettes and surroundings

La Peyne catchment, Southern France

Slope + Aspect Risk

1:25.000

Grid: UTM (WGS-1984 31T)

Sources:
BD Topo MNT. IGN PARIS - La Peyne (2001)
Top - Michelin Top 25 - 2643 OT (2001)
Bottom - Michelin Série Bleu - 2644 O (1990)

K.A. Gortmaker

January 5th, 2010

N

0 250 500 1,000 Meters

StudyArea

Slope + Aspect risk

High : 4

Low : 0

Utrecht University
Faculty of Geosciences
Department of Physical Geography

520000 521000 522000 523000 524000 525000 526000 527000 528000 529000

4827000 4826000 4825000 4824000 4823000 4822000 4821000

Lac des Olivettes and surroundings

La Peyne catchment, Southern France

Combined Hazard Map

1x vegetation | 1x human | 1x topo

1:25.000

Grid: UTM (WGS-1984 31T)

Sources:
BD Topo MNT. IGN PARIS - La Peyne (2001)
Top - Michelin Top 25 - 2643 OT (2001)
Bottom - Michelin Série Bleu - 2644 O (1990)

N

K.A. Gortmaker

June, 2010

Meters
0 250 500 1,000

520000 521000 522000 523000 524000 525000 526000 527000 528000 529000

4827000 4826000 4825000 4824000 4823000 4822000 4821000

StudyArea
Water

Fire Hazard
equal weights

High
Low

Utrecht University
Faculty of Geosciences
Department of Physical Geography

Combined hazard map (equal weights) - appendix O

Lac des Olivettes and surroundings

La Peyne catchment, Southern France

Combined Hazard Map

1x vegetation | 2/3 x human | 1/3 x topo

1:25.000

Grid: UTM (WGS-1984 31T)

Sources:
BD Topo MNT. IGN PARIS - La Peyne (2001)
Top - Michelin Top 25 - 2643 OT (2001)
Bottom - Michelin Série Bleu - 2644 O (1990)

N

K.A. Gortmaker

June, 2010

Meters
0 250 500 1,000

StudyArea
Water

Fire Hazard
1V + 0.66H + 0.33T
High
Low

Utrecht University
Faculty of Geosciences
Department of Physical Geography

520000 521000 522000 523000 524000 525000 526000 527000 528000 529000

4827000 4826000 4825000 4824000 4823000 4822000 4821000

Combined hazard map (weights 1 - 2/3 - 1/3) - appendix P

Lac des Olivettes and surroundings

La Peyne catchment, Southern France

Combined Hazard Map

1x vegetation | 3/5 x human | 1/5 x topo

1:25.000

Grid: UTM (WGS-1984 31T)

Sources:
BD Topo MNT. IGN PARIS - La Peyne (2001)
Top - Michelin Top 25 - 2643 OT (2001)
Bottom - Michelin Série Bleu - 2644 O (1990)

N

K.A. Gortmaker

June, 2010

Meters
0 250 500 1,000

520000 521000 522000 523000 524000 525000 526000 527000 528000 529000

4827000 4826000 4825000 4824000 4823000 4822000 4821000

StudyArea
Water

Fire Hazard

1V + 0.6H + 0.2T

High
Low

Utrecht University
Faculty of Geosciences
Department of Physical Geography

Combined hazard map (weights 1 - 3/5 - 1/5) - appendix Q